

# Theory of nonuniform electronic systems. I. Analysis of the gradient approximation and a generalization that works

David C. Langreth

Rutgers University, New Brunswick, New Jersey 08903

John P. Perdew

Tulane University, New Orleans, Louisiana 70118

(Received 6 November 1979)

A complete wave-vector analysis has been made of the gradient coefficient for the exchange-correlation energy of a nonuniform electronic system. It is shown that the majority of the contribution comes from a very small but universal region of  $k$  space near the origin. From this it can be concluded that random-phase-approximation-like calculations, like the present one or that of Rasolt and Geldart, which treat this region correctly, are likely to provide accurate results for the gradient coefficient and hence for the energy and structure of a system whose density is truly slowly varying. However, it also shows that the criterion for the validity of the gradient approximation itself is much more severe than previously supposed, so that the usual type of application, to say a surface or bulk material, is incorrect. For the surface case this is verified in unequivocal detail. On the other hand, a generalization of the gradient scheme based on an average slope instead of a local slope is proposed. This gives good agreement with limiting cases where they exist, and rough agreement with the interpolation scheme proposed previously by the authors.

## I. INTRODUCTION

Several years ago, we developed<sup>1,2</sup> a method of analyzing the exchange-correlation energy ( $E_{xc}$ ) for a metallic surface according to the "wave vector" of the dynamic density fluctuations contributing to it. In the process we concluded that the local-density approximation<sup>3</sup> (LDA) gave reasonable accuracy for the energy of such a system; this conclusion was also reached by others<sup>4</sup> at about the same time. We showed that the LDA became exact at large wave vector, but very poor at small wave vector. We then used a simple interpolation method to connect the two known regions, and hence to obtain the correction to the LDA (Fig. 1). This scheme has several obvious disadvantages. First, although it looked reasonable and agreed with various limiting cases, it was to a certain extent arbitrary; it would be much preferable to have a physically based calculational method for the intermediate wave-vector regime. Second, it was designed to pick up only the known long-wavelength error in the LDA; it implicitly assumed that there was no large error in the LDA in the intermediate regime; i.e.,  $k_{1T} \leq k \leq 2k_F$ . Our proof of the correctness of the LDA at large  $k$  only held rigorously for  $k \geq 2k_F$ , so the question of the intermediate region was worrisome. (Here  $k_{1T}$  and  $k_F$  are the Fermi-Thomas and Fermi wave vectors, respectively.) The third disadvantage was operational; it was difficult to implement the scheme in practice, and it was not even clear how to do so for an arbitrary nonuniform system.

It would seem as if there were an obvious method

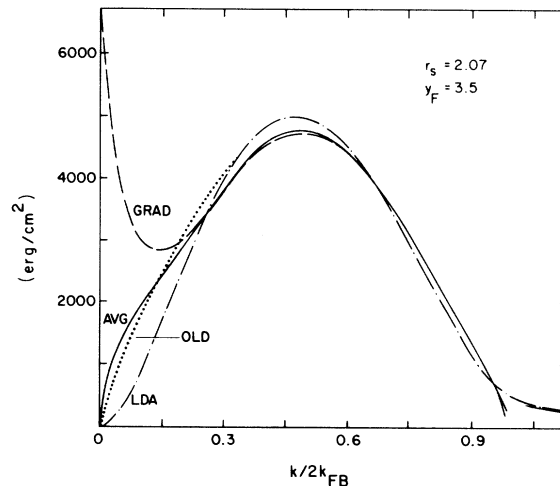


FIG. 1. Wave-vector analysis of the RPA exchange-correlation energy of the jellium surface ( $r_s = 2.07$ ) with a realistic density profile ( $y_F = 3.5$ ). The area under each curve is the exchange-correlation energy in the corresponding approximation. Dash-dotted curve (LDA): the local-density approximation. Dashed curve (GRAD): LDA plus second-order gradient correction. Solid curve (AVG): the new scheme proposed in this paper (LDA + Gaussian average-slope correction with  $p = 1.2$ , as defined later). Dotted curve (OLD): our old interpolation between the LDA and the exact  $k \rightarrow 0$  limit. In further figures we plot only the deviation from the LDA; that is, the difference between the dash-dotted curve in this figure and the approximation under consideration. Although this deviation, when integrated, is generally only a fairly small fraction of the exchange-correlation contribution, it is often a much larger fraction of the total energy.

already existing to calculate the deviation from the LDA that apparently had none of the above disadvantages. This is the gradient expansion<sup>3,5-7</sup> which provides a rigorous and systematic method for calculating the energy and density of a system whose spatial rate of density variation is sufficiently slow:

$$E_{xc}[n] = \int d^3r A_{xc}(n(\vec{r})) + \int d^3r B_{xc}(n(\vec{r})) |\nabla n(\vec{r})|^2 + \dots \quad (1.1)$$

Since the LDA [the leading term in Eq. (1.1)] is reasonably good for a surface, should not the application of the first gradient correction to  $E_{xc}$  [the second term in (1.1)] improve things considerably? It is certainly easy to implement in practice. The only question seemed to be that the gradient coefficient [ $B_{xc}(n)$ ] itself was difficult to calculate and various estimates differed from each other, although in our mind even this question was settled by the painstaking calculation of Rasolt and Geldart<sup>6</sup> (RG). Nevertheless, because we knew there were large corrections percentagewise to the LDA in the long-wavelength regime, we suspected that the gradient expansion would also produce large corrections there, so that the argument for the validity of the gradient approximation was really only specious. In fact, by comparing various limiting cases, we were able previously<sup>8</sup> to come to some negative conclusions concerning the validity of the gradient expansion for surfaces.

To investigate more fully the whole question of the corrections to the LDA, we present here<sup>9-11</sup> a complete wave-vector analysis of the first gradient correction for the exchange-correlation energy  $E_{xc}$ . We develop a new random-phase approximation (RPA) form for the gradient coefficient, but which is nearly the same as that of RG, and which involves the same physics. We make a wave-vector analysis of this form and find as we expected that the predominant contribution comes in the long-wavelength region, which we show to be universal. This enables us to conclude that the present calculation of the gradient coefficient and that of the RG (which ours was modeled after) are probably very reliable, because within the context of the second-order gradient expansion, they both accurately contain the contribution of the "gradient mode" which dominates this region, and which is treated exactly.

On the other hand, we show unambiguously, by comparison with the exact limiting form at long wavelength for a surface,<sup>1,2</sup> that the second-order gradient expansion is completely incorrect for a surface (Fig. 1), unless the profile varies so slowly as to be completely unphysical. We also

present evidence (not nearly so strong) that the gradient approximation is also invalid in practice for other physical systems of interest. (It appears that the gradient term gives the right correction to LDA only when  $\nabla n/n \ll \frac{1}{5} k_{FT}$ .)

Our wave-vector analysis of the gradient coefficient, however, also allows some important positive conclusions. The first is that it makes only a fairly small contribution in the intermediate wave-vector region where we expect it to be accurate (Fig. 1). Thus an implicit assumption in our earlier interpolation scheme is verified. But now we can make a further improvement, by interpolating between the intermediate- and long-wavelength deviations from the LDA, that is, between the gradient approximation at intermediate wavelength and the exact form at long wavelength. We develop a generalization of the gradient approximation, based on a mean slope rather than the local slope, in order to do this (Figs. 1 and 2). The scheme is still not an *a priori* calculation in the interpolation region, but is physically motivated and seems only weakly dependent on the exact way in which it is done. It goes smoothly from the exact calculations on a rapidly varying surface<sup>12</sup> to the gradient approximation for a very slowly varying one.

The remaining objection is that at present the method is still not easy to implement in a practical calculation on a real system. We are now working on a simplification of the method, which will allow

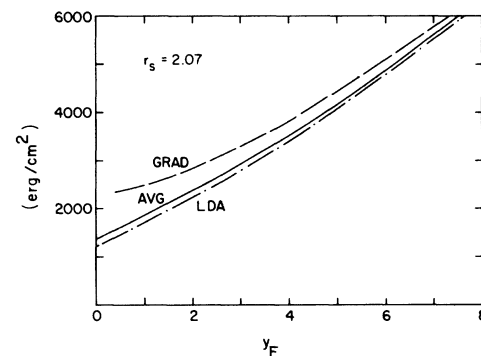


FIG. 2. Exchange-correlation energy of a metal surface ( $r_s = 2.07$ ) in RPA. Dash-dotted curve (LDA): the local density approximation. Dashed curve (GRAD): LDA plus second-order gradient correction. Solid curve (AVG): the new scheme proposed in this paper (LDA + Gaussian average-slope correction with  $p = 1.2$ , as defined later).  $y_F$  is the parameter of the class of density profiles of the linear potential model:  $y_F = 0$  is the infinite-barrier model,  $y_F = 3.25$  is a physical density profile for the jellium surface, and  $y_F = 8$  is a slowly varying profile. For comparison, the total surface energy of jellium ( $r_s = 2.07$ ) with a physical profile in RPA-LDA is  $-534$  erg/cm<sup>2</sup> (Ref. 8).

for easy application not only to surfaces, but also to other systems as well, and we will present these results in the future.

The organization of the paper is as follows: In Sec. II we review the wave-vector decomposition of the exchange-correlation energy  $E_{xc}$ , describe the density-functional version of the RPA, and apply the latter to derive formal expressions for the wave-vector analysis of  $E_{xc}$  in the electronic system of nearly uniform density, from which in the slowly varying limit we obtain the wave-vector decomposition of the LDA and the gradient correction. We also discuss the extent to which these results should persist beyond RPA-like theories. In Sec. III we present calculable expressions for the wave-vector-decomposed gradient coefficient. In Sec. IV we discuss how this tensor coefficient depends on the magnitude and direction of the wave vector (and on the electron density), identify the dominant term in it (corresponding to the "gradient mode") which peaks up strongly at small wave vector, and argue for the "universality" (beyond RPA) of this small wave-vector peak. In Sec. V we consider the wave-vector analysis of the gradient correction to the energy of model metallic surfaces. We give an analytic estimate of its small wave-vector behavior, which we compare (unfavorably) to the exact small wave-vector behavior, and we describe how *unphysically* slow the spatial density variation must be before the gradient term starts to give the right correction to the LDA. Finally, in Sec. VI we describe the reasons for the failure of the gradient correction at small wave vector, argue that at intermediate and small wave vector the local density gradient should be replaced by an average slope (averaged over the spatial extent of the "gradient mode"), and present the results of this average-slope scheme for model metallic surfaces.

## II. DERIVATION OF THE WAVE-VECTOR DECOMPOSITION

Here we show fully the derivation of the wave-vector decomposition of the gradient correction, which was sketched in our earlier Letter.<sup>10</sup> Relevant work has also been done by Rasolt and Geldart<sup>9</sup> (RG) and Peuckert.<sup>13</sup> As with all this work, our basic approximation could be described as the random-phase approximation for the energy within a density-functional context. We will define what we mean by this later. Although this approximation differs in only a slight way from RG (Ref. 6), a completely different formulation was necessary. This is because the relevant wave vector, as we have shown, is the Fourier transform variable of the density-density correlation function, and there

was no intermediate wave vector in RG (Ref. 6) corresponding to this; one cannot just "unsum" their equations. In addition, their " $\eta$  process" did not seem readily amenable to wave-vector decomposition. The Peuckert calculation,<sup>13</sup> on the other hand, although containing the correct wave vector  $\vec{k}$ , contained approximations at an early stage whose validity was difficult to judge, and was thus not useful for our purposes. Thus the complete reformulation which we sketched in our earlier Letter<sup>10</sup> was necessary.

We begin with an expression<sup>1,2,14</sup> for the exchange-correlation energy of an electronic system, obtained by switching on the electron-electron interaction adiabatically via a coupling constant  $g$ , while holding the electron density profile  $n(\vec{r})$  fixed:

$$E_{xc} = \frac{1}{2} \int d^3r \int d^3r' \frac{e^2}{|\vec{r} - \vec{r}'|} \times \int_0^1 dg \left( \frac{N}{\Omega} S_g(\vec{r}, \vec{r}') - n(\vec{r}) \delta(\vec{r} - \vec{r}') \right), \quad (2.1)$$

where

$$\frac{N}{\Omega} S_g(\vec{r}, \vec{r}') = \langle [n_{op}(\vec{r}) - n(\vec{r})][n_{op}(\vec{r}') - n(\vec{r}')] \rangle_g \quad (2.2)$$

is the density-density correlation function, and  $n_{op}(\vec{r})$  is the density operator. The nominal volume of the system,  $\Omega$ , encloses just the  $N$  electrons we are interested in, with periodic boundary conditions. As usual<sup>14</sup> we can interpret the result of the  $g$  integration in (2.1) as the product of  $n(\vec{r})$  with the density  $\rho(\vec{r}, \vec{r}')$  of the exchange-correlation hole around an electron at  $\vec{r}$ , so that  $E_{xc}$  is half the sum of the electrostatic interaction of each electron with its positively charged hole. From the definition (2.2) and conservation of particle number we have

$$\int d^3r' \rho(\vec{r}, \vec{r}') = -1, \quad (2.3)$$

so the electron and its hole together made a neutral object. Writing  $e^2/|\vec{r} - \vec{r}'|$  as a Fourier integral leads to the wave-vector decomposition defined earlier<sup>1,2</sup>:

$$E_{xc} = \frac{1}{\Omega} \sum_{\vec{k}} E_{xc}(\vec{k}) = \int \frac{d^3k}{(2\pi)^3} E_{xc}(\vec{k}), \quad (2.4)$$

where

$$E_{xc}(\vec{k}) = \frac{1}{2} \frac{4\pi e^2}{k^2} \int_0^1 dg N[S_g(\vec{k}) - 1]. \quad (2.5)$$

Physically, this says that dynamic density fluctuations of different size  $|\vec{k}|^{-1}$  contribute separately to  $E_{xc}$ . We define  $S_g(\vec{k})$  and many other quantities

by the Fourier-transform conventions

$$F(\vec{k}, \vec{k}') = \frac{1}{\Omega} \int d^3r \int d^3r' e^{-i(\vec{k}\cdot\vec{r} - \vec{k}'\cdot\vec{r}')} F(\vec{r}, \vec{r}'), \quad (2.6)$$

$$F(\vec{k}) = F(\vec{k}, \vec{k}), \quad (2.7)$$

$$G_{\vec{k}} = \int d^3r e^{-i\vec{k}\cdot\vec{r}} G(\vec{r}). \quad (2.8)$$

For some purposes it is convenient to define an average structure factor

$$\bar{S}(k) = \int_0^1 dg \int \frac{d\vec{k}}{4\pi} S_g(\vec{k}), \quad (2.9)$$

which is easily shown to be

$$\bar{S}(k) = \frac{1}{N} \int d^3r n(\vec{r}) \int d^3R e^{i\vec{k}\cdot\vec{R}} [\delta(\vec{R}) + \rho_{\text{sph}}(\vec{r}, R)], \quad (2.10)$$

the average over all electrons of the Fourier transform of the instantaneous density of an electron at  $\vec{r}$  plus its spherically averaged exchange-correlation hole  $\rho_{\text{sph}}$ . As Gunnarsson and Lundqvist<sup>14</sup> have pointed out in arguments intended to justify the local-density approximation, it is only this spherical average which counts in  $E_{\text{xc}}$ . Now (2.5) becomes

$$E_{\text{xc}} = \int_0^\infty dk \frac{4\pi k^2}{(2\pi)^3} N[\bar{S}(k) - 1] \frac{1}{2} \frac{4\pi e^2}{k^2}. \quad (2.11)$$

For example, we often write the exchange-correlation contribution to the metallic surface energy as

$$\sigma_{\text{xc}} = \int_0^\infty \frac{dk}{2k_{\text{FB}}} \gamma(k), \quad (2.12)$$

where  $k_{\text{FB}}$  is the bulk Fermi wave vector and  $\gamma(k)$  is  $2e^2 k_{\text{FB}}/\pi$  times the surface contribution per unit area to  $N\bar{S}(k)$ . It is  $\gamma(k)$  that was displayed in Fig. 1. In earlier work<sup>1,2</sup> we derived the exact small- $k$  limit

$$\gamma(k) \rightarrow \frac{k_{\text{FB}}}{4\pi} (\omega_s - \frac{1}{2}\omega_p) k \quad (2.13)$$

(taking  $\hbar=1$ ), where  $\omega_p = (4\pi n e^2/m)^{1/2}$  is the bulk and  $\omega_s = \omega_p/\sqrt{2}$  the surface plasmon frequency. Since the bulk contribution to  $N\bar{S}(k)$  is  $\propto k^2$ , Eq. (2.13) also gives the complete small- $k$  limit of  $N\bar{S}(k)$ . Whereas in the bulk (and neglecting Friedel oscillations) the hole  $\rho_{\text{sph}}(\vec{r}, R)$  is exponentially localized around its electron, with a characteristic size comparable to the Fermi-Thomas screening length, the hole becomes more diffuse near the surface.<sup>15</sup> Indeed by Fourier transformation we find that the  $k \rightarrow 0$  limit (2.13) implies that  $\rho_{\text{sph}}(\vec{r}, R)$  for  $\vec{r}$  in the surface region has a nonoscillatory long-range ( $R^{-4}$ ) tail from the plasmons. Thus the effect of the surface is to make the total exchange-

correlation energy less negative.

According to density-functional theory<sup>3</sup> (or rather a slight extension of it), we may expand (2.5), when the density  $n(\vec{r})$  varies slowly in space, as

$$E_{\text{xc}}(\vec{k}) = \int d^3r [A_{\vec{k}}^{\text{xc}}(n(\vec{r})) + \vec{\nabla}n(\vec{r}) \cdot \vec{B}_{\vec{k}}^{\text{xc}}(n(\vec{r})) \cdot \vec{\nabla}n(\vec{r}) + \dots]. \quad (2.14)$$

Here the first term is the wave-vector decomposition of the local-density approximation (LDA) which was discussed in Ref. 2:

$$A_{\vec{k}}^{\text{xc}}(n) = \frac{1}{2} \frac{4\pi e^2}{k^2} n[\bar{S}_u(k, n) - 1], \quad (2.15)$$

where  $\bar{S}_u(k, n)$  is the average structure factor of a uniform electron gas of density  $n$  (see Fig. 2 of Ref. 2). The tensor  $\vec{B}_{\vec{k}}^{\text{xc}}(n)$  is the wave-vector decomposition of the second-order gradient correction, which we deal with here. Since (2.14) must hold true, in particular, for a system of nearly uniform density, it follows that  $A_{\vec{k}}^{\text{xc}}$  and  $\vec{B}_{\vec{k}}^{\text{xc}}$  are functions only of the local density, and that the second term in the integrand can depend on no angle but that between  $\vec{k}$  and  $\nabla n$ ; i.e.,  $\vec{B}_{\vec{k}}^{\text{xc}}$  involves only one longitudinal ( $\hat{k}\hat{k}$ ) and one transverse coefficient. What makes it possible for us to calculate  $\vec{B}_{\vec{k}}^{\text{xc}}$  is the fact that the energy to order  $(\nabla n)^2$  can be calculated rigorously<sup>5</sup> in a hypothetical system, initially of uniform density, in which the density gradient is induced by a weak perturbation and the energy is carried to second order in this perturbation.

Before setting up the perturbation theory, we pause to make two general observations about (2.11): (1) The region of  $\vec{k}$  space near the origin, which would be heavily weighted by the  $4\pi e^2/k^2$  from the long-range Coulomb interaction, is unweighted by the three-dimensional phase-space volume element  $4\pi k^2 dk$ ; this is fortunate, since both the LDA and the gradient expansion for  $\bar{S}(k)$  are wrong at small  $k$ . [For example, in Fig. 1 we can compare the small- $k$  behavior of the LDA ( $\propto k^2$ ) and the gradient correction ( $\propto k^0$ ) with the exact behavior ( $\propto k$ ) for a metal surface.] (2) Equation (2.2) implies that  $\bar{S}(k=0) = 0$ , which also follows from the sum rule (2.3). We also expect that the exchange-correlation hole around an electron will be sufficiently localized so that  $\lim_{k \rightarrow 0} \bar{S}(k) = 0$ , with the limit achieved when  $k$  becomes small compared to the inverse of some microscopic length such as the Fermi-Thomas screening length, and not merely when  $k$  becomes small compared to the inverse of the size of the system. This expectation is satisfied by the

LDA (Refs. 1, 2, and 14) and also by our exact limit (2.13) for the metal surface, but *not* by the gradient expansion, as we saw in Fig. 1; this is a first indication that the gradient expansion is even more seriously wrong than the LDA in the  $k \rightarrow 0$  limit.

In order to evaluate the ground-state exchange-correlation energy of a real (spin-unpolarized) electronic system from (2.1), we need to know the density-density correlation function for a whole series ( $0 \leq g \leq 1$ ) of hypothetical systems having the same density profile  $n(\vec{r})$  but differing electron-electron interactions:

$$V(\vec{r} - \vec{r}') = ge^2/|\vec{r} - \vec{r}'|. \quad (2.16)$$

As  $g$  decreases from its real value of 1, we have to turn on a "*deus ex machina*" potential to hold the density profile  $n(\vec{r})$  fixed. At  $g=0$  we have a system of noninteracting electrons moving in a potential  $v^{\text{KS}}(\vec{r})$  which is the sum of this *deus ex machina* potential plus whatever external potential was present in the real system, so

$$n(\vec{r}) = \sum_{\alpha,s} f_{\alpha} |\psi_{\alpha}(\vec{r})|^2, \quad (2.17)$$

where

$$[-\nabla^2 + v^{\text{KS}}(\vec{r})]\psi_{\alpha}(\vec{r}) = \epsilon_{\alpha}\psi_{\alpha}(\vec{r}) \quad (2.18)$$

and  $f_{\alpha}$  is the zero-temperature Fermi-Dirac function. (Our units are such that  $2m = \hbar = 1$ ; although we sometimes write  $e^2$  explicitly, we also take  $e^2 = 2$  so that distances are measured in Bohrs and energies in rydberg.) Equations (2.17) and (2.18) are just the Kohn-Sham (KS) equations<sup>3</sup> of density-functional theory, and can be written down, with the *same*  $v^{\text{KS}}(\vec{r})$ , for any  $g$ ; at  $g=1$ , the only contributions to  $v^{\text{KS}}(\vec{r})$  are the external potential of the real system and the self-consistent local electrostatic and exchange-correlation potentials<sup>3</sup> from the electrons.

To evaluate the energy from (2.1), we use the zero-temperature limit of the fluctuation-dissipation theorem<sup>16</sup>:

$$\begin{aligned} \frac{N}{\Omega} S_{\rho}(\vec{r}, \vec{r}') &= \int_{-\infty}^{\infty} \frac{d\omega}{2\pi} e^{-i\omega t} \frac{N}{\Omega} S_{\rho}(\vec{r}, \vec{r}', \omega) |_{t=0} \\ &= -\frac{1}{\pi} \int_0^{\infty} d\omega \text{Im} \chi(\vec{r}, \vec{r}', \omega) \\ &= \frac{1}{2\pi i} \int_c d\omega \chi(\vec{r}, \vec{r}', \omega), \end{aligned} \quad (2.19)$$

where the dynamic susceptibility  $\chi$ , which depends implicitly on  $g$ , gives the linear response  $\delta n$  of the system (at interaction strength  $g$ ) to a weak external perturbation  $\delta v^{\text{ext}}$  oscillating with frequency  $\omega$ ,

$$\delta v^{\text{ext}}(\vec{r}, t) = \delta v^{\text{ext}}(\vec{r}, \omega) e^{-i\omega t} e^{\zeta t} + \text{c.c.}, \quad (2.20)$$

where  $\zeta = 0^+$ . The contour  $c$  in (2.19) encloses the positive real axis in the positive sense. We abbreviate

$$\delta n(\vec{r}, \omega) = \int d^3r' \chi(\vec{r}, \vec{r}', \omega) \delta v^{\text{ext}}(\vec{r}', \omega) \quad (2.21)$$

as

$$\delta n = \chi \delta v^{\text{ext}}, \quad (2.22)$$

in an obvious matrix notation which can be used in real or Fourier space.

In order to use (2.19), we need to evaluate the dynamic susceptibility  $\chi$  of a nonuniform many-electron system. We can make progress by defining a screened potential,

$$\delta v^{\text{scr}}(\vec{r}, \omega) = \delta v^{\text{ext}}(\vec{r}, \omega) + \int d^3r' V(\vec{r} - \vec{r}') \delta n(\vec{r}', \omega) \quad (2.23)$$

or

$$\delta v^{\text{scr}} = \delta v^{\text{ext}} + V \delta n, \quad (2.24)$$

and a function  $\bar{\chi}(\vec{r}, \vec{r}', \omega)$  which gives the system's response to  $\delta v^{\text{scr}}$ :

$$\delta n = \bar{\chi} \delta v^{\text{scr}}. \quad (2.25)$$

Equations (2.22), (2.24), and (2.25) have the solution

$$\chi = \bar{\chi} (1 - V \bar{\chi})^{-1}. \quad (2.26)$$

So far, no approximation has been made, except the assumption of adiabatic connection between the ground states of the noninteracting ( $g=0$ ) and fully interacting ( $g=1$ ) systems, and this assumption is hardly questionable for the system of nearly uniform density which will be our main interest here.

To progress further, we must approximate  $\bar{\chi}$  in (2.26). We make the RPA; i.e., we replace  $\bar{\chi}$  by  $\chi_0$ , which is what  $\bar{\chi}$  and  $\chi$  reduce to when  $g=0$ .  $\chi_0$  is the dynamic susceptibility of a system of noninteracting electrons with density profile  $n(\vec{r})$ . By evaluating the standard expression<sup>16</sup> for  $\chi$  with Slater-determinant wave functions, or simply by applying time-dependent perturbation theory to the independent motion of each electron, we find

$$\begin{aligned} \chi_0(\vec{r}, \vec{r}', \omega) &= \sum_{\alpha, \alpha', s} \frac{f_{\alpha} - f_{\alpha'}}{\omega + i\zeta + \epsilon_{\alpha} - \epsilon_{\alpha'}} \\ &\quad \times \psi_{\alpha}^*(\vec{r}) \psi_{\alpha'}(\vec{r}) \psi_{\alpha'}^*(\vec{r}') \psi_{\alpha}(\vec{r}'), \end{aligned} \quad (2.27)$$

where  $\psi_{\alpha}$  are the Kohn-Sham one-electron wave functions of (2.18). The approximation for the energy based on (2.1), (2.19) and

$$\chi \simeq \chi_0 (1 - V \chi_0)^{-1} \quad (2.28)$$

is what we mean by "RPA in a density-functional context."

Now recall that to evaluate the gradient coefficient  $\bar{B}_{\vec{k}}^{\text{xc}}(n)$  of Eq. (2.14), we only need the exchange-correlation energy to second order in the deviation from a system of uniform density [in which  $v^{\text{KS}}(\vec{r})=0$ ]. We expand (2.27) to second order in  $v^{\text{KS}}(\vec{r})$  as

$$\chi_0 = \chi_{0u} + \chi_1 + \chi_2, \quad (2.29)$$

where

$$\chi_{0u}(\vec{r}, \vec{r}', \omega) = \frac{1}{\Omega} \sum_{\vec{k}} e^{i\vec{k} \cdot (\vec{r} - \vec{r}')} \chi_{0u}(\vec{k}, \omega), \quad (2.30)$$

$$\chi_{0u}(\vec{k}, \omega) = \frac{1}{\Omega} \sum_{\vec{k}, s} \frac{f_{\vec{k}} - f_{\vec{k}+\vec{k}}}{\omega + i\zeta + \epsilon_{\vec{k}} - \epsilon_{\vec{k}+\vec{k}}}$$

is the usual Lindhard susceptibility for a system of noninteracting electrons of uniform density, and  $\epsilon_{\vec{k}} = K^2$ . The first- and second-order terms in (2.29) are

$$\chi_1 = \int d^3r_1 \frac{\delta \chi_0(\vec{r}, \vec{r}', \omega)}{\delta v^{\text{KS}}(\vec{r}_1)} \Big|_{v^{\text{KS}}=0} v^{\text{KS}}(\vec{r}_1), \quad (2.31)$$

$$\chi_2 = \frac{1}{2} \int d^3r_1 \int d^3r_2 \frac{\delta^2 \chi_0(\vec{r}, \vec{r}', \omega)}{\delta v^{\text{KS}}(\vec{r}_1) \delta v^{\text{KS}}(\vec{r}_2)} \Big|_{v^{\text{KS}}=0} \times v^{\text{KS}}(\vec{r}_1) v^{\text{KS}}(\vec{r}_2). \quad (2.32)$$

Note that the functional derivatives above are to be taken at constant particle number. We need the expansion to second order in  $v^{\text{KS}}$  of

$$\chi = (\chi_{0u} + \chi_1 + \chi_2)(1 - V\chi_{0u} - V\chi_1 - V\chi_2)^{-1}. \quad (2.33)$$

We assume (with no loss in generality) that the contribution to the energy of (2.1) which is first order in  $v^{\text{KS}}$  vanishes, i.e., that  $\int d^3x v^{\text{KS}}(\vec{x}) = 0$ . Then, neglecting the first-order piece of  $\chi$  (which is irrelevant for the energy) we find that (2.33) becomes

$$\chi \simeq \chi_{0u}(1 - V\chi_{0u})^{-1} + (1 - \chi_{0u}V)^{-1} \chi_2 (1 - V\chi_{0u})^{-1} + (1 - \chi_{0u}V)^{-1} \chi_1 (1 - V\chi_{0u})^{-1} V\chi_1 (1 - V\chi_{0u})^{-1}. \quad (2.34)$$

Equation (2.34) is simplest in Fourier space, where  $V$  and  $\chi_{0u}$  are diagonal. We follow the Fourier-transform conventions of (2.6)–(2.8) and apply translational invariance arguments [i.e., the functional derivatives in (2.31) and (2.32) must be invariant under an arbitrary equal displacement of all spatial arguments] to find that the needed quantities take the form

$$\chi_1(\vec{k}, \vec{k} + \vec{q}, \omega) = \frac{2}{\Omega} \Lambda_{\vec{k}, \vec{q}}^{\uparrow}(\omega) v_{-\vec{q}}^{\text{KS}}, \quad (2.35)$$

$$\chi_2(\vec{k}, \omega) = \frac{1}{\Omega^2} \sum_{\vec{q}} B_{\vec{k}, \vec{q}}^{\uparrow}(\omega) |v_{\vec{q}}^{\text{KS}}|^2. \quad (2.36)$$

[Note that only the diagonal of the transform of  $\chi_2$  is needed in (2.34).] The coefficients  $\Lambda$  and  $B$  could be found by expanding the expression (2.27) for  $\chi_0$  to second order in  $v^{\text{KS}}$  by ordinary time-independent one-particle perturbation theory. Time-reversal symmetry tells us that  $\Lambda_{\vec{k}, \vec{q}}^{\uparrow}(\omega) = \Lambda_{-\vec{k} - \vec{q}, \vec{q}}^{\uparrow}(\omega)$ , while the inversion symmetry of the uniform system gives  $\Lambda_{\vec{k}, \vec{q}}^{\uparrow}(\omega) = \Lambda_{-\vec{k}, -\vec{q}}^{\uparrow}(\omega)$ . Now (2.34) becomes

$$\chi(\vec{k}, \omega) \simeq \chi_{0u}(\vec{k}, \omega) / \epsilon(\vec{k}, \omega) + \frac{1}{\epsilon^2(\vec{k}, \omega)} \frac{1}{\Omega^2} \sum_{\vec{q}} [B_{\vec{k}, \vec{q}}^{\uparrow}(\omega) + 4\Lambda_{\vec{k}, \vec{q}}^{\uparrow}(\omega) V_{\vec{k} + \vec{q}} / \epsilon(\vec{k} + \vec{q}, \omega)] |v_{\vec{q}}^{\text{KS}}|^2, \quad (2.37)$$

where

$$\epsilon(\vec{k}, \omega) = 1 - V_{\vec{k}} \chi_{0u}(\vec{k}, \omega) \quad (2.38)$$

and

$$V_{\vec{k}} = 4\pi e^2 g / k^2. \quad (2.39)$$

Note that  $\epsilon$  depends implicitly on  $g$ , since  $V_{\vec{k}}$  does.

To get an expression resembling the gradient expansion (2.14), we need to eliminate  $v_{\vec{q}}^{\text{KS}}$  from (2.37) in favor of  $\Delta n_{\vec{q}}$ , the Fourier transform of

$$\Delta n(\vec{r}) = n(\vec{r}) - \frac{N}{\Omega}, \quad (2.40)$$

where  $n(\vec{r})$  is given by (2.17). This we can do without approximation, since rigorously  $\Delta n(\vec{r})$  is given by applying time-independent perturbation theory for  $\psi$  to Eq. (2.18), treating  $v^{\text{KS}}$  as a weak perturbation, with the result

$$\Delta n_{\vec{q}} = \chi_{0u}(\vec{q}, 0) v_{\vec{q}}^{\text{KS}}. \quad (2.41)$$

We find, after substituting (2.41) into (2.37), and the result into the double-equal-wave-vector Fourier transform of (2.19), and the result of that into (2.5), that

$$E_{xc}(\vec{k}) = -\frac{1}{2} \frac{4\pi e^2}{k^2} N + \frac{1}{2} \int_0^1 \frac{dg}{g} \Omega \int_c \frac{d\omega}{2\pi i} \left[ \frac{\chi_{0u}(\vec{k}, \omega) V_{\vec{k}}}{\epsilon(\vec{k}, \omega)} + \frac{1}{\Omega^2} \sum_{\vec{q}} \left( \frac{B_{\vec{k}, \vec{q}}^{\rightarrow}(\omega) V_{\vec{k}}}{\epsilon^2(\vec{k}, \omega)} + 4\Lambda_{\vec{k}, \vec{q}}^2(\omega) \frac{V_{\vec{k}+\vec{q}}}{\epsilon(\vec{k}+\vec{q}, \omega)} \frac{V_{\vec{k}}}{\epsilon^2(\vec{k}, \omega)} \right) \times [\chi_{0u}(\vec{q}, 0)]^{-2} |\Delta n_{\vec{q}}|^2 \right]. \quad (2.42)$$

The *only* coupling-constant dependence in the large square bracket of (2.42) is in  $V_{\vec{k}}$  which is either exhibited explicitly or occurs implicitly in  $\epsilon$  [see Eq. (2.38)]. Therefore the  $g$  integration is easily performed and one finds for our system of nearly uniform density

$$E_{xc}(\vec{k}) = E_{xc}^{\text{uniform}}(\vec{k}) + \frac{1}{\Omega} \sum_{\vec{q}} K_{xc}(\vec{k}, \vec{q}) |\Delta n_{\vec{q}}|^2, \quad (2.43)$$

where

$$E_{xc}^{\text{uniform}}(\vec{k}) = -\frac{1}{2} \frac{4\pi e^2}{k^2} N - \frac{1}{2} \Omega \int_c \frac{d\omega}{2\pi i} \ln \epsilon(\vec{k}, \omega) \quad (2.44)$$

is the wave-vector decomposition in RPA of the exchange-correlation energy of the uniform electron gas of density  $N/\Omega$ . [Note that  $\epsilon(\vec{k}, \omega)$  is now and hereafter given by Eqs. (2.38) and (2.39) but with  $g=1$ ; it is *not* the exact dielectric function of the uniform electron gas.] What is of more interest, we find in (2.43) that

$$K_{xc}(\vec{k}, \vec{q}) = \frac{1}{2} \int_c \frac{d\omega}{2\pi i} [B_{\vec{k}, \vec{q}}^{\rightarrow}(\omega) \mathcal{U}(\vec{k}, \omega) + 2\Lambda_{\vec{k}, \vec{q}}^2(\omega) \mathcal{U}(k, \omega) \mathcal{U}(\vec{k}+\vec{q}, \omega) D(y)] \chi_{0u}^2(\vec{q}, 0), \quad (2.45)$$

where

$$\mathcal{U}(\vec{k}, \omega) = 4\pi e^2/k^2 \epsilon(\vec{k}, \omega) \quad (2.46)$$

and

$$D(y) = \frac{2(1+y)}{y} \left( 1 - \frac{1}{y} \ln(1+y) \right) \quad (2.47)$$

with

$$y = \epsilon(\vec{k}+\vec{q}, \omega)/\epsilon(\vec{k}, \omega) - 1. \quad (2.48)$$

Note that  $K_{xc}(\vec{k}, \vec{q})$  contains two terms: a ‘‘Hartree-Fock-type’’ term with one factor of the screened interaction  $\mathcal{U}$ , and a ‘‘fluctuation’’ term with two factors of  $\mathcal{U}$ .

If the small deviation  $\Delta n(\vec{r})$  of the density from uniformity is also slowly varying in space, (2.43) may be expanded in powers of  $q$ . We follow Ma and Brueckner<sup>5</sup> by comparing the small  $q$  expansion of (2.43) with the small  $\Delta n$  expansion of (2.14). We find that the wave-vector decomposition of the LDA is

$$A_{\vec{k}}^{xc}(n) = -\frac{1}{2} \frac{4\pi e^2}{k^2} n - \frac{1}{2} \int_c \frac{d\omega}{2\pi i} \ln \epsilon(\vec{k}, \omega), \quad (2.49)$$

as anticipated in (2.15), while the wave-vector decomposition of the gradient correction is

$$\vec{B}_{\vec{k}}^{xc}(n) = \frac{1}{2} \nabla_{\vec{q}}^{\rightarrow} \nabla_{\vec{q}}^{\leftarrow} K_{xc}(\vec{k}, \vec{q})|_{q=0}. \quad (2.50)$$

We also note for completeness that

$$K_{xc}(\vec{k}, 0) = \frac{1}{2} \frac{\partial^2}{\partial n^2} A_{\vec{k}}^{xc}(n). \quad (2.51)$$

Equations (2.45) and (2.50) comprise the basic

equations of this paper.

The factor  $D(y)$  appears in (2.45) specifically because  $\vec{k}$  is defined to be the same  $\vec{k}$  as in Eq. (2.5), and hence the same wave vector used in our earlier work, and for which the various limit theorems derived there apply.  $D(y)$  may be replaced by unity in the integral  $\sum_{\vec{k}} K_{xc}(\vec{k}, \vec{q})$ , which is the relevant quantity for obtaining the total gradient coefficient rather than its wave-vector decomposition. (To see this, simply make the change of summation variable  $\vec{k} \rightarrow -\vec{k}' - \vec{q}$  and apply the symmetries of the uniform system.) We would have missed the factor  $D(y)$  entirely if we had tried to guess the wave-vector decomposition from RG (Ref. 6) rather than deriving it from (2.1).

Although our expression (2.45) for  $K_{xc}(\vec{k}, \vec{q})$  was derived from our density-functional version of RPA, the Kohn-Sham potential  $v^{\text{KS}}$  canceled out completely, leaving a result that is identical to what would be found from the simple or lowest-order RPA diagrams for the energy, or equivalently from the ‘‘time-dependent Hartree approximation’’ for the density response. In the remainder of this section, we will discuss the extent to which this kind of cancellation is a general feature of the exact  $K_{xc}(\vec{k}, \vec{q})$ .

To this end, we give a diagrammatic interpretation of our approximation. First note that  $\mathcal{U}(\vec{k}, \omega) = V_{\vec{k}}^{\rightarrow}/\epsilon(\vec{k}, \omega)$  is the RPA screened interaction, i.e., the bare Coulomb interaction  $V_{\vec{k}}^{\rightarrow}$  divided by the RPA dielectric function [see Fig. 3(b)].  $B_{\vec{k}, \vec{q}}^{\rightarrow}(\omega)$  is a second functional derivative of

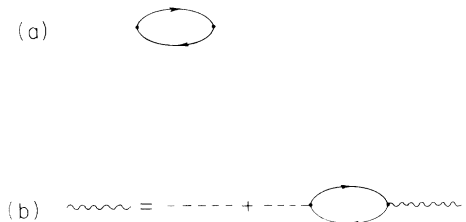


FIG. 3. (a) Density response to an already screened potential in the RPA. If the solid lines represent the propagators in the full nonuniform system, then this represents  $\chi_0$ ; if the solid lines are uniform system propagators then it represents  $\chi_{0u}$ . (b) The equation which determines  $\mathcal{U}$ . Here  $\mathcal{U}$  is the wiggly line,  $V_k \equiv 4\pi e^2/k^2$  is the dashed line, and the bubble represents  $\chi_{0u}$  as in the second case above.

the density response function [see Fig. 3(a)]. The integral of the first term in the square brackets of (2.45) can thus be represented by diagrams of the type shown in either Figs. 4(a) or 4(b), depending where the derivatives are taken. The quantity  $\Lambda_{\vec{k}, \vec{q}}^{\pm}(\omega)$  is the lowest-order triangular vertex three interactions, so that the integral of the second term in the square brackets of (2.45) is the sum of the two (equal) diagrams of Fig. 4(c), and includes the factor  $D(y)$  as discussed earlier.

It might seem on the surface that this result does not account for the higher-order diagrams

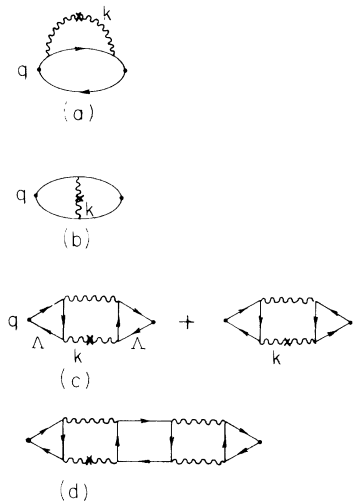


FIG. 4. (a) and (b) are diagrams for the  $B_{\vec{k}, \vec{q}}(\omega)$  of Eq.(2.36). The derivatives with respect to  $v$  are taken at the corners. The  $\times$  means that the sum over internal momentum  $\vec{k}$  is not performed at this point. (c) The contribution  $2\Lambda_{\vec{k}, \vec{q}}^2 \mathcal{U}(\vec{k}, \omega) \mathcal{U}(\vec{k} + \vec{q}, \omega)$ . (d) A higher-order diagram that is included approximately in our treatment.

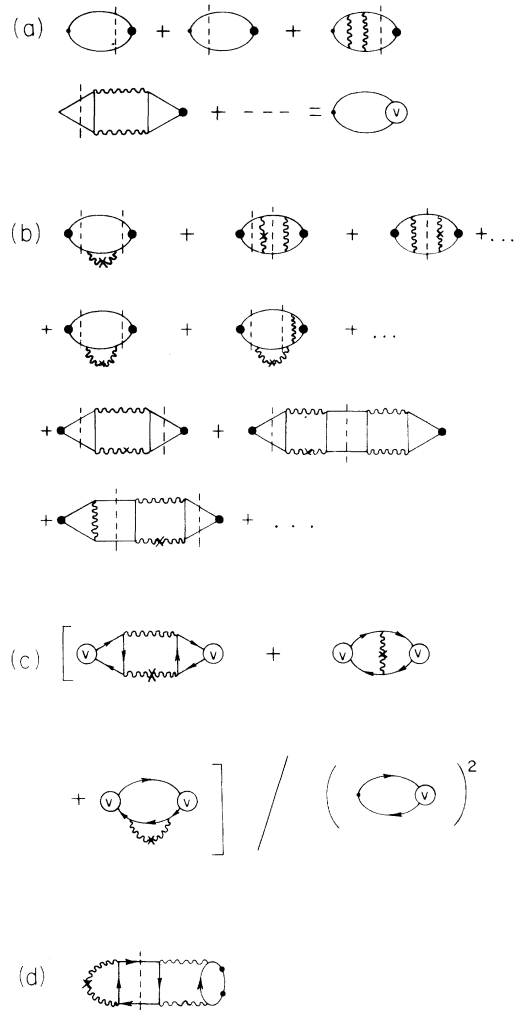


FIG. 5. (a) Typical diagrams for the density response  $\delta n_{\vec{q}}$  to an already screened potential  $v_{\vec{q}}^{\text{scr}}$  represented by the solid dot. The contribution to the right of the vertical dashed line is the contribution to the total Coulomb exchange-correlation potential  $v$ . Arrows are omitted from the electron lines for simplicity. (b) Diagrams for  $\chi - \chi_{0u} / \epsilon$ . Contributions to the left of the first or to the right of the second vertical dashed line sum to the nonlocal Coulomb-exchange-correlation potential  $v$ . (c) Diagram combination occurring in  $K_{xc}(\vec{k}, \vec{q})$ . The diagrams in the numerator are the sum of the diagrams in (b) above [note that there are two diagrams each of the type of the first and third in the numerator in (c), but we have included but one each for brevity]. The quantity which is squared in the numerator is the sum of the diagrams of the type (a) above. (d) A diagram of the type that occurs in the full shielded potential approximation. The part to the right of the dashed line is a many-body interference term between the two screened potentials. Such terms are not included in the summation above, but are eliminated in our approximation by the assumption of the existence of a local exchange-correlation potential.

which would occur, for example, in the Kadanoff and Baym shielded potential approximation,<sup>17</sup> and which make an important contribution to  $\bar{\chi}$  of Eq. (2.25). These are the terms which RG (Ref. 6) try to account for with their “ $\eta$  process.” For example, if Fig. 4(c) is large, should not Fig. 4(d) be at least non-negligible? To see that these higher-order diagrams have been approximately accounted for, we go back to (2.37) and (2.41).

Consider first (2.41). Recall that  $v_q^{\text{KS}}$  is the effective or Kohn-Sham potential induced in an initially uniform system by an external static potential  $v_q^{\text{ext}}$  [which is not to be confused with the later, time-dependent perturbation  $\delta v^{\text{ext}}(\vec{r}, \omega)$ ]. If we define a local, static screened potential  $v_q^{\text{scr}} = v_q^{\text{ext}} + V \Delta n_q$ , where  $\Delta n_q$  is the density response to  $v_q^{\text{ext}}$ , then  $\Delta n_q$  is expanded as in Fig. 5(a), where the solid dot represents  $v^{\text{scr}}$ . The sum of the terms to the right of the dashed line represents a many-body screened potential, called  $v$  in Fig. 5(a). It naturally comes out of the normal perturbation expansion as a nonlocal potential, but we know that, at least with respect to the calculation of a static density as in (2.41), we may redefine things so that it may be replaced by a local potential; i.e., we simply define

$$v_q^{\text{KS}} = v_q^{\text{scr}} \bar{\chi}_u(\vec{q}, 0) / \chi_{0u}(\vec{q}, 0), \quad (2.52)$$

where  $\bar{\chi}_u(\vec{q}, 0)$  is the irreducible polarization part of the susceptibility of the uniform system [a special case of (2.25)]. Equation (2.41) can therefore be made exact, as is well known from density-functional theory. Note that  $v_q^{\text{KS}} / v_q^{\text{scr}}$  differs non-negligibly from unity, and at small  $q$  is equal to  $(1 - \eta)^{-1}$ , i.e., to the ratio  $\kappa / \kappa_0$  of the compressibility of a neutralized interacting uniform electron gas to that of a noninteracting one, which diverges when  $r_s$  gets as large as six or so.<sup>16</sup>

Consider now the diagrammatic expansion of  $\chi(\vec{k}, \omega) - \chi_{0u}(\vec{k}, \omega) / \epsilon(\vec{k}, \omega)$ , although not necessarily in the approximation (2.37). Typical diagrams that would occur in the full shielded potential approximation<sup>17</sup> are shown in Fig. 5(b). Again the solid dot represents the screened external potential  $v^{\text{scr}}$ , while the  $\times$  denotes the place where there is a missing factor of  $V_{\vec{k}}$  and where  $\vec{k}$  is not summed over. The parts of Fig. 5(b) to the right of the right dashed vertical line and to the left of the left dashed line can be summed into a (non-local and time-dependent) many-body screened potential  $v$ . The diagrams contributing to  $v$  in Fig. 5(b) are the same as those contributing to  $v$  in Fig. 5(a). The quantity  $K_{\text{sc}}(\vec{k}, \vec{q})$  [see Eq. (2.43)] is then given by the sum of diagrams 5(b) divided by that of 5(a) squared; this is shown in Fig. 5(c).

We see that the effective potential  $v$  tends to cancel. Indeed in the approximation (2.45) it gets

eliminated exactly. This is because we can generate our approximation (2.45) from the diagram of Fig. 5(c) if we replace the nonlocal  $v$  by the *same* local potential in both the numerator and the denominator. Since the local potential then cancels out, it does not matter what we take it to be; in the usual derivation of RPA as a “time-dependent Hartree approximation,” i.e., in the usual lowest-order diagrammatic RPA, this local potential turns out to be  $v^{\text{scr}}$ , while in our density-functional version of RPA it turns out to be  $v^{\text{KS}}$ . Although in the full shielded potential theory we can rigorously have the local potential  $v^{\text{KS}}$  in the denominator via (2.52), there is no way to redefine things in all the terms of the numerator so that  $v$  is the same local potential as in the denominator. In addition, there is the somewhat related problem of many-body interference terms between  $v$ 's in diagrams where the  $v$ 's share the same propagator lines [see Fig. 5(d)].

It is thus clear that our treatment of the higher-order terms consists in assuming that the many-body screened potential  $v$  can be replaced by the same local, static potential ( $v^{\text{KS}}$  or  $v^{\text{scr}}$ ) wherever it appears. In an exact theory this potential cancels from the problem only approximately. We make the approximation that the cancellation is exact. Note that the corrections to either the numerator or the denominator of (2.45) are of the order of  $(1 - \eta)^{-2}$ ; it is this principal effect of the higher-order corrections that cancels. Our treatment of the higher-order terms is thus very similar to that of RG,<sup>6</sup> who approximate various sums of many-body diagrams by their compressibility or small- $q$  analogs, and who find a similar cancellation of the  $(1 - \eta)^{-2}$  terms. In their method there is a remnant, considerably smaller than  $(1 - \eta)^{-2}$ , which fails to cancel. Whether this extra remnant (which makes roughly a 10% correction to the gradient coefficient at  $r_s = 2$ ) should be present is a question which is probably beyond the state of the art to answer, as one would not be hard pressed to produce other terms of the same size. In the absence of convincing evidence, we tend to prefer our approximation because it follows clearly from the density-functional version of RPA, without the need for intricate argumentation. Nevertheless, the important conclusions of this paper do not hinge on this question.

Finally we conclude by mentioning that all the results of this section could have been (and indeed originally were) derived directly from the rules of many-body perturbation theory, without any appeal to the Kohn-Sham<sup>3</sup> formalism. We have presented our results in the language of the latter to make contact with the area where we suspect most of the applications of our work will be.

## III. EVALUATION

To obtain the wave-vector analysis of the gradient coefficient  $B_{xc}$  we must expand  $K_{xc}(\vec{k}, \vec{q})$  in (2.45) to second order in  $q$  according to (2.50). There are a number of ways to do this, all of which are long and tedious. We chose the finite-temperature diagram technique,<sup>18</sup> and made the Taylor-series expansion directly in the diagrams. There are two sources of  $q^2$  terms in (2.45): (1) the  $q^2$  term from the expansion of the square brackets times  $\chi_{0u}^{-2}(0, 0)$  and (2) the terms in the square brackets evaluated at  $q=0$ , times the  $q^2$  term in the expansion of  $\chi_{0u}^{-2}(q, 0)$ . We consider first terms of type (1). Later we will consider the (simpler) terms of type (2) which we call the compressibility terms because they comprise the wave-vector analysis of the compressibility coefficient  $\eta$ .

We define the fluctuation term as

$$F_{\vec{k}}^{\vec{q}}(\vec{q}) = \int_c \frac{d\omega}{2\pi i} \Lambda_{\vec{k}, \vec{q}}^2(\omega) \mathcal{U}(\vec{k}, \omega) \mathcal{U}(\vec{k} + \vec{q}, \omega) D(\nu), \quad (3.1)$$

and the Hartree-Fock-type term as

$$H_{\vec{k}}^{\vec{q}}(\vec{q}) = \int_c \frac{d\omega}{2\pi i} B_{\vec{k}, \vec{q}}^{\vec{q}}(\omega) \mathcal{U}(\vec{k}, \omega). \quad (3.2)$$

We expand these, as well as  $\chi_{0u}(q, 0)$  in powers of  $q$ :

$$\begin{aligned} F_{\vec{k}}^{\vec{q}}(\vec{q}) &= F_{\vec{k}}^{\vec{q}(0)} + F_{\vec{k}}^{\vec{q}(2)} + \dots, \\ H_{\vec{k}}^{\vec{q}}(\vec{q}) &= H_{\vec{k}}^{\vec{q}(0)} + H_{\vec{k}}^{\vec{q}(2)} + \dots, \\ \chi_{0u}(q, 0) &= \chi_{0u}^{(0)} + \chi_{0u}^{(2)} + \dots, \end{aligned} \quad (3.3)$$

where the superscript ( $n$ ) indicates the order in  $q$  (e.g.,  $F_{\vec{k}}^{\vec{q}(2)} \sim q^2$ , etc.). Therefore

$$\begin{aligned} \vec{q} \cdot \vec{B}_{\vec{k}}^{xc} \cdot \vec{q} &= \frac{1}{2} (\chi_{0u}^{(0)})^{-2} [(2F_{\vec{k}}^{\vec{q}(2)} + H_{\vec{k}}^{\vec{q}(2)}) \\ &\quad - (2\chi_{0u}^{(2)}/\chi_{0u}^{(0)})(2F_{\vec{k}}^{\vec{q}(0)} + H_{\vec{k}}^{\vec{q}(0)})]. \end{aligned} \quad (3.4)$$

The first terms in the square brackets are the lengthiest, and we consider them first.

In an analogous manner to (3.3), we expand

$$\Lambda = \Lambda^{(0)} + \Lambda^{(1)} + \Lambda^{(2)} + \dots, \quad (3.5a)$$

and defining

$$W_{\vec{k}}^{\vec{q}}(\vec{q}) = \mathcal{U}(\vec{k} + \vec{q}, \omega) D(\nu) \quad (3.5b)$$

we expand

$$W = W^{(0)} + W^{(1)} + W^{(2)}. \quad (3.5c)$$

In terms of these quantities the fluctuation term is then

$$\begin{aligned} F_{\vec{k}}^{(2)} &= \int_c \frac{d\omega}{2\pi i} W^{(0)} [2\Lambda^{(0)} \Lambda^{(2)} W^{(0)} + (\Lambda^{(1)})^2 W^{(0)} \\ &\quad + 2\Lambda^{(0)} \Lambda^{(1)} W^{(1)} + (\Lambda^{(0)})^2 W^{(2)}]. \end{aligned} \quad (3.6)$$

We evaluate  $\Lambda$  (and later a number of other quantities) directly from the diagrams in terms of the frequency-dependent response functions of the electron gas.

To this end we define

$$\begin{aligned} P^+(k, \omega) &= \frac{1}{\Omega} \sum_{\vec{k}_s} \frac{f_{\vec{k}+\vec{k}}}{\omega - \epsilon_{\vec{k}+\vec{k}} + \epsilon_{\vec{k}}} \\ &= \frac{1}{2\pi^2} \int_{-1}^1 dx \int_0^{k_F} dK K^2 \frac{1}{\omega - 2Kkx - k^2} \end{aligned} \quad (3.7)$$

and

$$P^-(k, \omega) = \frac{1}{\Omega} \sum_{\vec{k}_s} \frac{-f_{\vec{k}+\vec{k}}}{\omega - \epsilon_{\vec{k}+\vec{k}} + \epsilon_{\vec{k}}}. \quad (3.8)$$

We note that  $P^+(k, \omega) = P^-(k, -\omega)$ . We also define

$$P(k, \omega) = P^+(k, \omega) + P^-(k, \omega), \quad (3.9)$$

$$\bar{P}(k, \omega) = P^+(k, \omega) - P^-(k, \omega). \quad (3.10)$$

$P(k, \omega)$  is the frequency-dependent density response function of the uniform system (diagrammatically a single bubble of two bare propagators) and  $P(q, \omega + i\xi) = \chi_{0u}(q, \omega)$ . It should be clear by inspection of the diagrams of Fig. 4 that most of the expansion of  $\Lambda$  and  $B$  in (3.5) can be obtained by taking various derivatives of  $P$ . The places where this was not possible were then isolated, and (3.7), (3.8), and (3.10) were then used to express the latter as derivatives of  $\bar{P}$ .

In this manner we obtain

$$\Lambda^{(0)} = -\frac{1}{2} \frac{\partial P}{\partial \mu}, \quad (3.11)$$

where  $\mu$  is the chemical potential (in the absence of  $\nu_{\vec{q}}^{KS}$ ). Similarly, we find

$$\Lambda^{(1)} = -\frac{1}{4} (\vec{q} \cdot \vec{\nabla}_{\vec{k}}) \frac{\partial P}{\partial \mu} \quad (3.12)$$

and

$$\begin{aligned} \Lambda^{(2)} &= -\frac{1}{12} (\vec{q} \cdot \vec{\nabla}_{\vec{k}})^2 \frac{\partial P}{\partial \mu} + \frac{1}{12} q^2 \frac{\partial^2 P}{\partial \mu^2} - \frac{1}{6} q^2 \frac{\partial^2 \bar{P}}{\partial \mu \partial \omega} + \frac{1}{6} q^2 \frac{\partial^2 P}{\partial \omega^2}. \end{aligned} \quad (3.13)$$

The expansions for  $\mathcal{U}$  and  $D$ , on the other hand, are obtained directly from their defining expressions (2.46), (2.47), (2.38), and (3.5).

Before writing the results for  $F$ , it is convenient to define some dimensionless quantities, and in the process split the various tensor quantities into

their longitudinal and transverse components. We let  $x = k/2k_F$ , where  $k_F$  is the Fermi wave vector,  $\vec{Q} \equiv \vec{q}/2k_F$ ,  $s^2 = k_{FT}^2/(2k_F)^2$ ; where  $k_{FT}$  is the Fermi-Thomas wave vector ( $k_{FT}^2 = 2e^2 k_F/\pi$ ). Our units are always such that  $\hbar = 2m = 1$ . We also let

$$W^{(0)} = (2\pi^2 s^2/k_F) w_0, \quad (3.14)$$

$$W^{(1)} = (2\pi^2 s^2/k_F) \vec{Q} \cdot \hat{k} w_1, \quad (3.15)$$

$$W^{(2)} = (2\pi^2 s^2/k_F) [(\vec{Q} \times \hat{k})^2 w_2^t + (\vec{Q} \cdot \hat{k})^2 w_2^l], \quad (3.16)$$

$$\Lambda^{(0)} = (1/32\pi^2 k_F) \lambda_0, \quad (3.17)$$

$$\Lambda^{(1)} = (1/32\pi^2 k_F) \vec{Q} \cdot \hat{k} \lambda_1, \quad (3.18)$$

$$\Lambda^{(2)} = (1/32\pi^2 k_F) [(\vec{Q} \times \hat{k})^2 \lambda_2^t + (\vec{Q} \cdot \hat{k})^2 \lambda_2^l], \quad (3.19)$$

where  $\hat{k}$  is a unit vector in the  $\vec{k}$  direction. Similarly we define a dimensionless form for  $F$ :

$$F_{\vec{k}}^{(2)} = -(s^2/64\pi k_F^2) [(\vec{Q} \times \hat{k})^2 f_2^t + (\vec{Q} \cdot \hat{k})^2 f_2^l]. \quad (3.20)$$

Finally, in anticipation of deforming the contour  $c$  in (3.1) and (3.2) so it runs up the imaginary axis, we define  $\gamma = -i(2k_F)^{-2}\omega$ .

Upon substituting (3.14)–(3.20) into (3.6), we obtain

$$f_2^t = s^2 \int_0^\infty dy (2\lambda_0 w_0^2 \lambda_2^t + \lambda_0^2 w_0 w_2^t), \quad (3.21)$$

$$f_2^l = s^2 \int_0^\infty dy (2\lambda_0 w_0^2 \lambda_2^l + \lambda_0^2 w_0^2 + 2\lambda_0 \lambda_1 w_0 w_1 + \lambda_0^2 w_0 w_2^l). \quad (3.22)$$

The analytic expressions for the  $\lambda$ 's are a straightforward but tedious consequence of performing the derivatives indicated in (3.11)–(3.13), using the expressions for the  $P$ 's given in (3.7)–(3.10). The  $w$ 's are obtained directly by expanding their definition [see (3.5)] in powers of  $q$ , using (2.46) and (2.47). Both above results are lengthy and are listed in Appendix A.

We now turn to the Hartree-Fock-type term  $H_{\vec{k}}^{(2)}$  which is the second-order expansion of (3.2). Here are two slight technical complications that arise. The first is that the integration contour that occurs naturally in the finite-temperature perturbation technique is not the contour  $c$ , but rather the one which surrounds the poles of the Bose function  $(e^{\beta\omega} - 1)^{-1}$ . If the integrand [in our case  $\tilde{B}_{\vec{k},\vec{q}}^{(2)\mu}(\omega)\mathcal{U}(k,\omega)$ ] goes to zero sufficiently rapidly at large  $|\omega|$ , then the contour may be shifted to one which becomes equal to  $c$  as the zero-temperature limit is taken. However, for the Hartree-Fock term [ $\mathcal{U}(k,\omega) = V_{\vec{k}}$ ] this sufficiently rapid vanishing does not occur, and there is an extra contribution when the contour is shifted. We thus replace (3.2) by

$$H_{\vec{k}}^{(2)}(\vec{q}) = \int_c \frac{d\omega}{2\pi i} \tilde{B}_{\vec{k},\vec{q}}^{(2)\mu}(\omega)\mathcal{U}(k,\omega) + \tilde{H}_{\vec{k}}^{(2)}(\vec{q}), \quad (3.23)$$

where  $\tilde{B}$  is  $B$  as evaluated by the usual diagram technique, and  $\tilde{H}$  is the extra contribution from shifting the contour.

The second complication is that the diagram technique fixes the chemical potential  $\mu$ , rather than the particle number  $N$ . It is thus most convenient to evaluate functional derivatives at constant  $\mu$ , and then add a term to account for the changes in  $\mu$ . Since  $\int d^3r v^{KS}(\vec{r}) = 0$ , this problem occurs only in second-order functional derivatives, as in  $B$ . This complication is actually less annoying here than in the zero-temperature diagram technique, where it occurs as a nonequivalence of  $\epsilon$  and  $\mu$  derivatives of the single-particle Green's function (see Ref. 5, Appendix A). We define this extra chemical potential shift term  $C$  by replacing (3.23) by

$$H_{\vec{k}}^{(2)}(\vec{q}) = H_{\vec{k}}^{(2)\mu}(\vec{q}) + C_{\vec{k}}^{(2)}(\vec{q}), \quad (3.24)$$

$$H_{\vec{k}}^{(2)\mu}(\vec{q}) = \int_c \frac{d\omega}{2\pi i} \tilde{B}_{\vec{k},\vec{q}}^{(2)\mu}(\omega)\mathcal{U}(k,\omega) + \tilde{H}_{\vec{k}}^{(2)\mu}(\vec{q}), \quad (3.25)$$

where  $\tilde{B}_{\vec{k},\vec{q}}^{(2)\mu}$  is the same as  $\tilde{B}_{\vec{k},\vec{q}}$  except the derivatives with respect to  $v^{KS}$  [see (2.31) and (2.32)] are evaluated at fixed  $\mu$  instead of fixed  $N$ .

First consider  $H_{\vec{k}}^{(2)\mu}$ , and in analogy with (3.3) let

$$\begin{aligned} H_{\vec{k}}^{(2)\mu}(\vec{q}) &= H_{\vec{k}}^{(0)\mu} + H_{\vec{k}}^{(2)\mu}, \\ \tilde{B}_{\vec{k},\vec{q}}^{(2)\mu}(\omega) &= \tilde{B}_{\vec{k},\vec{q}}^{(0)\mu}(\omega) + \tilde{B}_{\vec{k},\vec{q}}^{(2)\mu}(\omega), \\ \tilde{H}_{\vec{k}}^{(2)\mu} &= \tilde{H}_{\vec{k}}^{(0)\mu} + \tilde{H}_{\vec{k}}^{(2)\mu}, \end{aligned} \quad (3.26)$$

where, as usual, the numerical superscript indicates the order in  $q$ . Then using the same kinds of manipulations that lead to (3.11)–(3.13), we find from the diagrams of Fig. 4 that

$$\begin{aligned} \tilde{B}_{\vec{k}}^{(2)\mu}(\omega) &= \frac{1}{12} \left( \frac{1}{2}(\vec{q} \cdot \vec{\nabla}_{\vec{k}})^2 \frac{\partial^2 P}{\partial \mu^2} - q^2 \frac{\partial^3 P}{\partial \mu^3} \right. \\ &\quad \left. + q^2 \frac{\partial^3 \bar{P}}{\partial \mu^2 \partial \omega} - q^2 \frac{\partial^3 P}{\partial \mu \partial \omega^2} \right) \end{aligned} \quad (3.27)$$

and

$$\tilde{H}_{\vec{k}}^{(2)} = -q^2 V_{\vec{k}} / (96\pi^2 k_F^3). \quad (3.28)$$

Again we separate the longitudinal and transverse components and introduce dimensionless quantities:

$$\begin{aligned} \tilde{B}_{\vec{k}}^{(2)\mu}(\omega) &= [1/64\pi^2 (2k_F)^3] [(\vec{Q} \cdot \hat{k})^2 b_2^l + (\vec{Q} \times \hat{k})^2 b_2^t], \\ \tilde{H}_{\vec{k}}^{(2)\mu} &= -(s^2/64\pi k_F^2) [(\vec{Q} \cdot \hat{k})^2 h_2^l + (\vec{Q} \times \hat{k})^2 h_2^t]. \end{aligned} \quad (3.29)$$

Then one finds

$$h_2^l = \int_0^\infty dy w_0 b_2^l + \tilde{h}_2, \quad (3.30a)$$

$$h_2^t = \int_0^\infty dy w_0 b_2^t + \tilde{h}_2. \quad (3.30b)$$

Evaluating the derivatives in (3.27) results in lengthy analytic expressions for  $b_2^i$  and  $b_2^t$ , and these are listed in Appendix A, along with the expression for  $\bar{h}_2$ .

We now turn to the chemical potential shift term  $C_k^*(\bar{q})$  in (3.24). In order to keep the particle number constant when the effective potential  $v^{KS}$  is applied, the chemical potential must shift by an amount  $\delta\mu$  given by the average over the unperturbed Fermi sphere of the second-order correction  $\delta\epsilon_k^*$  to the Kohn-Sham eigenvalue:

$$\begin{aligned}\delta\mu &= \frac{1}{\Omega^2} \sum_q J_q^* |v_q^{KS}|^2 \\ &= \frac{1}{\Omega^2} \sum_q \left( \frac{J_q^*}{[\chi_{0u}(q, 0)]^2} \right) |\Delta n_{\bar{q}}|^2,\end{aligned}\quad (3.31)$$

where

$$J_q^* = \frac{\pi^2}{k_F} \frac{\partial}{\partial \mu} \chi_{0u}(q, 0), \quad (3.32)$$

Then, following the conventions of Eqs. (2.45) and (3.2),  $C_k^*(\bar{q})$  is given by

$$\frac{2}{\Omega} J_q^* \frac{\partial E_{xc}^{\text{uniform}}(\bar{k})}{\partial \mu}, \quad (3.33)$$

where  $E_{xc}^{\text{uniform}}(k)$  is the wave-vector decomposition of the uniform electron gas [see Eq. (2.44)],

$$\frac{\partial E_{xc}^{\text{uniform}}(\bar{k})}{\partial \mu} = \Omega s^2 \left( -\frac{1}{2x^2} + \frac{1}{4\pi} \int_0^\infty dy w_0 \lambda_0 \right). \quad (3.34)$$

Note that all the  $q$  dependence of (3.33) occurs in  $J_q^*$  and all the  $k$  dependence occurs in  $(\partial E/\partial \mu)$ . Let

$$C_k^*(\bar{q}) = C_k^{(0)} + C_k^{(2)} + \dots, \quad (3.35)$$

where as before the superscript indicates the order in  $q$ , and define

$$C_k^{(2)} = (s^2/64\pi k_F^2) [c_2^t(\bar{Q} \cdot \hat{k})^2 + c_2^t(\bar{Q} \times \hat{k})^2]. \quad (3.36)$$

The derivative in (3.32) is readily evaluated. In analogy to (3.30) we write (noting that  $c_2^t$  is trivially equal to  $c_2^t$ , and performing the Hartree-Fock part of the  $x$  integral analytically)

$$c_2^t = c_2^t = \int_0^\infty dy w_0 \bar{b}_2 + \bar{c}_2. \quad (3.37)$$

For uniformity, the quantities  $\bar{b}_2$  and  $\bar{c}_2$  are listed in Appendix A, Eqs. (A14) and (A15).

We now turn to the ‘‘compressibility’’ terms, that is, the last terms in the square brackets in (3.4). These are considerably simpler than the preceding second-order terms, but may be calculated in much the same way. The fluctuation term  $F_k^{(0)}$  is given by

$$F_k^{(0)} = \int_c \frac{d\omega}{2\pi i} [\mathcal{U}(k, \omega) \Lambda^{(0)}]^2, \quad (3.38)$$

where  $\Lambda^{(0)}$  is given by (3.11) and  $\mathcal{U}(k, \omega)$  by (2.46). For the Hartree-Fock-type term we expand (3.25) [see (3.26)], and then

$$H_k^{(0)\mu} = \int_c \frac{d\omega}{2\pi i} \mathcal{U}(k, \omega) \tilde{B}_k^{(0)\mu}(\omega) + \tilde{H}_k^{(0)}, \quad (3.39)$$

where

$$\tilde{B}_k^{(0)\mu}(\omega) = \frac{1}{2} \frac{\partial^2 P}{\partial \mu^2} \quad (3.40)$$

and

$$\tilde{H}_k^{(0)} = -(1/8\pi^2 k_F) V_k. \quad (3.41)$$

Because all the  $q$  dependence of the chemical potential shift term [ $C_k^*(\bar{q})$  of (3.33)] is in  $J_q^*$ , it is clear that  $C_k^{(2)}$  and  $C_k^{(0)}$  are related by  $Q^2$  times a numerical factor, and we find

$$C_k^{(0)} = 3C_k^{(2)}/Q^2. \quad (3.42)$$

Again we use reduced dimensionless quantities:

$$\begin{aligned}F_k^{(0)} &= (-s^2/64\pi k_F^2) f_0, \\ H_k^{(0)\mu} &= (-s^2/64\pi k_F^2) h_0^\mu, \\ C_k^{(0)} &= (-s^2/64\pi k_F^2) c_0.\end{aligned}\quad (3.43)$$

Then

$$f_0 = s^2 \int_0^\infty dy w_0^2 \lambda_0^2, \quad (3.44a)$$

$$h_0^\mu = \int_0^\infty dy w_0 b_0 + \bar{h}_0, \quad (3.44b)$$

$$c_0 = 3c_2^t = 3c_2^t, \quad (3.44c)$$

where  $w_0$  is given in Appendix A by (A11a),  $\lambda_0$  is given by (A1),  $c_2^t$  by (3.37), and

$$b_0 = 16x(1-x)/a - 16x(1+x)/b \quad (3.45)$$

and

$$\bar{h}_0 = 16\pi/x^2, \quad (3.46)$$

where  $a$  and  $b$  are given in Appendix A.

Since  $\chi_{0u}^{(0)}$  and  $-2\chi_{0u}^{(2)}/\chi_{0u}^{(0)}$  are easily evaluated as (in our units)  $-k_F/2\pi^2$  and  $2Q^2/3$ , respectively, we are now ready to put the pieces together into (3.4). We note first that the original decomposition (2.5) is normalized such that the total exchange correlation energy is given by (2.4). Therefore  $\tilde{B}_k^{xc}$  of Eq. (2.14) has similar normalization. We would rather define a  $\tilde{B}_k^*$  that has the same dimensions as  $B_{xc}$  of Eq. (1.1) (when dimensions are restored). We therefore let

$$\tilde{\beta}^{xc} \equiv \frac{4\pi x^2 (2k_F)^3}{(2\pi)^3} \tilde{B}_k^{xc}, \quad (3.47)$$

where  $x = k/2k_F$  as usual, and  $k_F \equiv k_F(\bar{F})$  is the local Fermi wave vector. The normalization is now such that

$$B_{xc} \bar{1} = \int_0^\infty dx \langle \bar{\beta}^{xc} \rangle, \quad (3.48)$$

where the angular brackets indicate an average over the direction of  $\bar{k}$ , and  $\bar{1}$  is the unit tensor. We now separate  $\bar{\beta}^{xc}$  into its tensor components and introduce dimensionless quantities:

$$\bar{\beta}^{xc}(\bar{x}) = \alpha \left[ Z_1(x) \frac{\bar{x}\bar{x}}{x^2} + Z_t(x) \left( \bar{1} - \frac{\bar{x}\bar{x}}{x^2} \right) \right], \quad (3.49)$$

where

$$\begin{aligned} \alpha &= \frac{1}{2} \left( \frac{1}{\chi_{0u}} \right)^2 \frac{1}{(2\pi)^3} \left( \frac{e}{2k_F} \right)^2 \\ &= \left( \frac{\pi}{16(3\pi^2)^{4/3}} \right) \frac{e^2}{n^{4/3}} = 2.14 \times 10^{-3} \frac{e^2}{n^{4/3}}, \end{aligned} \quad (3.50)$$

and where  $\bar{x} = \bar{k}/2k_F$ . Note that

$$\beta^{xc}(x) \bar{1} \equiv \langle \bar{\beta}^{xc}(\bar{x}) \rangle = \alpha Z(x) \bar{1}, \quad (3.51)$$

where

$$Z(x) = \frac{1}{3} Z_1(x) + \frac{2}{3} Z_t(x). \quad (3.52)$$

We find from (3.4) plus the various definitions of reduced quantities<sup>19</sup> that

$$\begin{aligned} Z_1(x) &= (-x^2/4\pi) [(2f_2^t + h_2^u + c_2^t) \\ &\quad + 2(2f_0 + h_0^u + c_0)/3] \end{aligned} \quad (3.53a)$$

and

$$\begin{aligned} Z_t(x) &= (-x^2/4\pi) [(2f_2^t + h_2^u + c_2^t) \\ &\quad + 2(2f_0 + h_0^u + c_0)/3]. \end{aligned} \quad (3.53b)$$

The expressions listed in Appendix A are in a form suitable to numerical evaluation of the  $y$  integrals, (3.21), (3.22), (3.30), (3.37), and (3.44), which determine  $Z_1$  and  $Z_t$  according to (3.53). Near  $x=1$  ( $k=2k_F$ ) further analytic work had to be done, as  $Z(x)$  has singularities at  $x=1$  which can be represented only by distributions and not by ordinary functions. Fortunately the coefficients of these distributions can be expressed analytically, and we find that for  $x \sim 1$  the leading terms are

$$\begin{aligned} Z_1(x) &\sim \frac{1}{3(1+s^2/2)} [3\delta(x-1) + \delta'(x-1)] \\ &\quad - \frac{s^2}{12(1+s^2/2)^2} \left( 3 \frac{d}{dx} [\text{sgn}(x-1) \ln|x-1|] \right. \\ &\quad \left. + \frac{d}{dx} \ln|x-1| - 2\delta(x-1) \right), \end{aligned} \quad (3.54a)$$

$$Z_t(x) \sim \frac{4}{3(1+s^2/2)} \delta(x-1). \quad (3.54b)$$

The Dirac  $\delta$  function and its derivative  $\delta'$  are familiar; so is  $(d/d\xi) \ln|\xi|$  which is just the principal-value integral of  $1/\xi$ . Perhaps less

familiar is the distribution  $(d/d\xi)(\text{sgn}\xi \ln|\xi|)$ . This, like the principal-value integral  $1/\xi$ , has a precursor on both sides of  $\xi=0$  proportional in magnitude to  $|1/\xi|$ . Unlike the principal-value integral, however, these precursors are *even* functions of  $\xi$ ; nevertheless, the integral over  $\xi$  is well defined because of an infinite negative contribution in the infinitesimal region around  $\xi \sim 0$  ( $x \sim 1$ ).

For completeness we note that the expressions (3.53), for the "Hartree-Fock-type term" when evaluated to the lowest order in  $e^2$ , constitute the wave-vector analysis of the gradient expansion for the exchange energy:

$$\{Z_1(x)\}_x = -4x\theta(1-x) + \delta(x-1) + \frac{1}{3}\delta'(x-1), \quad (3.55a)$$

$$\{Z_t(x)\}_x = -4x\theta(1-x) + \frac{4}{3}\delta(x-1) \quad (3.55b)$$

[where all the frequency integrals have been performed analytically in the complex plane by restoring the contour  $c$  of Eq. (2.19)].  $\{Z(x)\}_x$  has a very different structure from  $Z(x)$ ; in fact, the former vanishes at small  $x$  where the latter has a strong peak, as discussed in Sec. IV.

Finally, we can summarize the results of this section by writing the gradient coefficient of Eq. (1.1) as

$$B_{xc}(n) = e^2 C_{xc}(n)/n^{4/3}, \quad (3.56)$$

where

$$C_{xc}(n) = \frac{\pi}{16(3\pi^2)^{4/3}} \int_0^\infty dx Z(x) \quad (3.57)$$

and  $Z(x)$  is given by Eq. (3.52). For exchange alone, one has<sup>5</sup>  $C_x = -1.667 \times 10^{-3}$ , while for exchange and correlation  $C_{xc}$  is  $+2.568 \times 10^{-3}$  in the high-density limit<sup>5</sup> and does not deviate far from this at metallic densities<sup>6,10</sup> (see Appendix B).

#### IV. RESULTS AND DISCUSSION

The  $y$  integrals determining  $Z_1(x)$  and  $Z_t(x)$  were evaluated numerically using the expression listed in Appendix A. This was straightforward (but tedious) except for small  $x$  and  $x \sim 1$  where special care had to be taken. The results are shown in Fig. 6 for a given electronic density corresponding to  $r_s = 2$  ( $\frac{4}{3}\pi r_s^3 a_0^3 n \equiv 1$ ). The gradient coefficient itself is proportional to the weighted [see (3.52)] sum of the areas under the two curves, plus the extra contributions of the distributions near  $x=1$ . The gradient coefficient  $B_{xc}$  thus obtained was plotted vs  $r_s$  in Fig. 2 of Ref. 10. There we saw that the coefficient was very close to that of RG (Ref. 6); the only difference is the slightly different treatment of the higher-order terms in the two approaches. Note that the variation with density, once the leading  $n^{-4/3}$  dependence is factored out,

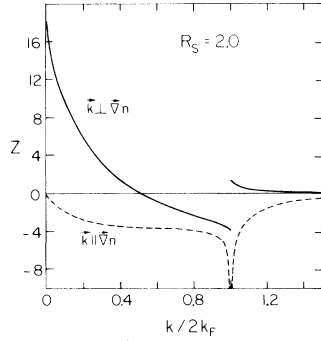


FIG. 6. Longitudinal (dashed line) and transverse (solid line) components of  $Z$  versus wave vector  $x = k/2k_F$ .

is rather slow, so that a major error would not be made if the high-density limit (for  $Z$ ) were to be used at all densities. If more accurate results are needed, we give an analytic fit to these results in Appendix B. Two words of warning are in order, however. The first is that although we believe our result (or that of RG) is an excellent estimate of the true gradient coefficient, we do not know of any examples of physically interesting systems where the density variation is slow enough for the gradient expansion to apply. As we saw from our previous account of the present work, it certainly does not apply to a metallic surface. Second, note the behavior of the  $Z$  coefficient at high density according to Fig. 2 of Ref. 10. The sharp depression as  $r_s \rightarrow 0$  is real; the gradient coefficient is very rapidly varying in a small region around  $r_s \sim 0$ . This means that, even though the value of  $Z$  at physical  $r_s$  values ( $2 \lesssim r_s \lesssim 6$ ) is not much different from the Ma and Brueckner<sup>5</sup> high-density results, a series expansion<sup>13</sup> of the gradient coefficient around  $r_s = 0$  is bound to fail to give accurate results in the physically interesting range of densities.

Returning now to the curves of Fig. 6, we see that most of the structure occurs at  $x \sim 1$  in  $Z_l$  and  $x \sim 0$  in  $Z_t$ . The sharp increase in  $|Z_l|$  at  $x \sim 1$  looks like a major contribution at first, but actually it is just the precursor of the distribution  $(d/dx)[\text{sgn}(x-1) \ln|x-1|]$ . Its weight is essentially canceled by the singular contributions right at  $x=1$ . The extent to which this cancellation occurs, however, is not evident until the wave-vector decomposition is integrated over a varying density; we will see this later.

The only important structure then is at  $x \sim 0$  in  $Z_t$ . This corresponds to a long-wavelength excitation traveling perpendicular to the density gradient. We will term this excitation a "gradient mode." We will find that this long-wavelength region in  $Z_t$  (note that  $Z_t$  is weighted twice as

much as  $Z_l$  in the energy) makes the predominant contribution to the gradient term in the exchange-correlation energy of a surface.

It is instructive to find out which of the many contributions gives this long-wavelength peak, and to evaluate this region analytically. Inspection of the  $k$  (or  $x$ ) dependence of (3.21), (3.30), (3.37), and (3.44) along with the corresponding expressions in Appendix A convinces one that the leading contributions at small  $k$  all come from the fluctuation term  $f$ . This is not inconsistent with the earlier finding of RG that the fluctuation term makes the largest total contribution in the high-density limit. Inspection of Fig. 4(c) makes it clear that this term is the energy of a bosonlike excitation (clearly becoming a plasmon as  $k \rightarrow 0$ ) which scatters twice off the potential from the density gradient.

We now evaluate  $f_2^t$  analytically as  $k \rightarrow 0$ . Referring to (3.21), (A1)–(A3), (A8), and (A11), we see that the leading contribution to  $f_2^t$  comes from

$$f_2^t \rightarrow s^2 \int_0^\infty dy \lambda_0^2 w_0 w_2^t. \quad (4.1)$$

Referring to (A11d), one sees further that the leading contribution to  $w_2^t$  is

$$w_2^t \rightarrow -1/x^4 \epsilon. \quad (4.2)$$

This is a key point, because it means that the only  $q$  dependence relevant for  $f_2^t$  originally came from the bare potential  $V_{\mathbf{k}+\mathbf{q}}^+$ ; therefore in obtaining the transverse contribution we need only  $\Lambda$ ,  $\epsilon$ , and  $D$  at zero  $q$  [see Eq. (3.1)].

At zero  $k$ , we have<sup>16</sup>

$$\epsilon = 1 - \omega_p^2/\omega^2 = 1 + s^2/3y^2 \quad (4.3)$$

and

$$\lambda_0 \rightarrow 4x^2/y^2. \quad (4.4)$$

Substitution in (4.1) gives

$$f_2^t \rightarrow -(12\pi\sqrt{3}/s)(1/x^2) \quad (4.5)$$

and

$$Z_t(0) \rightarrow 6\sqrt{3}/s. \quad (4.6)$$

Although it appears that several terms in the expansion (3.22) for  $f_2^t$  would contribute to this order, one finds that they cancel each other, so that

$$Z_l(0) = 0. \quad (4.7)$$

For  $r_s = 2$ , we find that (4.6) gives  $Z_t(0) = 18.04$ , which clearly agrees with the numerical evaluation shown in Fig. 6.

The results (4.6) and (4.7) are quite general (beyond RPA). It is clear that there will always be a "triangular" vertex [call it  $\bar{\Lambda}_{\mathbf{k},\mathbf{q}}^+(\omega)$ ] which is analogous to  $(v_q^{KS}/v_q^{scr})\Lambda_{\mathbf{k},\mathbf{q}}^+(\omega)$  of the RPA and which

connects at each corner to a screened potential line. Then there is always a fluctuation diagram representing the modified energy of the long-wavelength fluctuation, and which is given by [cf. (2.42)]

$$E_{xc}^{\text{fluct}}(\vec{k}) - \frac{1}{2} \int_0^1 \frac{dg}{g} \int_c \frac{d\omega}{2\pi i} 4\bar{\Lambda}_{\vec{k},\vec{q}}^2(\omega) \times \left( \frac{V_{\vec{k}+\vec{q}} V_{\vec{k}}}{[\bar{\epsilon}(\vec{k}+\vec{q},\omega)\bar{\epsilon}^2(\vec{k},\omega)]} \right) \times \bar{\chi}^{-2}(q,0) |\Delta n_{\vec{q}}|^2, \quad (4.8)$$

where now  $\bar{\epsilon}$  is the exact dielectric function

$$\bar{\epsilon}(\vec{k},\omega) = 1 - V_{\vec{k}} \bar{\chi}(q,\omega) \quad (4.9)$$

and  $\bar{\chi}(q,\omega)$  is the exact irreducible polarization part (for the uniform system). We want to evaluate (4.8) when  $k$  and  $q$  are both small. Rotational symmetry requires that<sup>20</sup>  $\bar{\Lambda}_{\vec{k},\vec{q}}^+(\omega) \propto \vec{k} \cdot (\vec{k} + \vec{q})$ , so that

$$\bar{\Lambda}_{\vec{k},\vec{q}}^+(\omega) = \bar{\Lambda}_{\vec{k},0}^+(\omega) \left( \frac{\vec{k} \cdot (\vec{k} + \vec{q})}{k^2} \right). \quad (4.10)$$

Furthermore, since  $\bar{\epsilon}(\vec{k},\omega)$  goes to a constant at small  $k$ , the leading contribution at small  $k$  and  $q$  comes from setting  $k$  and  $q=0$  in  $\bar{\epsilon}(\vec{k},\omega)$  and  $\epsilon(\vec{k}+\vec{q},\omega)$ . Similarly we may let  $q \rightarrow 0$  in  $\bar{\chi}(q,0)$ . Therefore

$$E_{xc}^{\text{fluct}}(\vec{k}) - \frac{1}{2} \int_0^1 \frac{dg}{g} \int_c \frac{d\omega}{2\pi i} 4[\bar{\Lambda}_{\vec{k},0}^+(\omega)/\bar{\chi}(0,0)]^2 \frac{V_{\vec{k}}^2}{\bar{\epsilon}^3(0,\omega)} \times \left( \frac{[\vec{k} \cdot (\vec{k} + \vec{q})]^2}{k^2(\vec{k} + \vec{q})^2} \right) |\Delta n_{\vec{q}}|^2. \quad (4.11)$$

Note that in  $\bar{\chi}(0,0)$  the  $\omega \rightarrow 0$  limit is taken first and that we have the rigorous equality

$$\bar{\chi}(0,0) = (\kappa/\kappa_0) \chi_{0u}(0,0), \quad (4.12)$$

where the compressibility enhancement factor  $\kappa/\kappa_0$  may also be written

$$\kappa/\kappa_0 = 1/(1-\eta) = \lim_{q \rightarrow 0} (v_q^{\text{KS}}/v_q^{\text{scr}}). \quad (4.13)$$

The ‘‘triangular’’ vertex  $\bar{\Lambda}$  is not ‘‘corner symmetric’’ in the limit  $k \rightarrow 0$ , because a finite frequency  $\omega$  goes into or out of two of the corners, but not the third. The former receive no many-body enhancement, but the third receives the compressibility enhancement, so that

$$\lim_{k \rightarrow 0} \bar{\Lambda}_{\vec{k},0}^+(\omega)/\Lambda_{\vec{k},0}^+(\omega) = \kappa/\kappa_0. \quad (4.14)$$

Thus the many-body corrections cancel numerator and denominator in the square brackets in (4.11). Finally in the  $k \rightarrow 0$  finite  $\omega$  limit, the exact  $\bar{\epsilon}(\vec{k},\omega)$  is still given by (4.3), whose coupling-constant dependence is given by

$$\epsilon = 1 - g\omega_p^2/\omega^2, \quad (4.15)$$

so that the integral over  $g$ , which is now contained only in  $\epsilon$  and  $V_{\vec{k}}$ , may be performed and one obtains for this contribution to  $K_{xc}(\vec{k},\vec{q})$  [see (2.43)]

$$K_{xc}(\vec{k},\vec{q}) \rightarrow \int_c \frac{d\omega}{2\pi i} \left( \frac{\Lambda_{\vec{k},0}^+(\omega) V_{\vec{k}}}{\epsilon(0,\omega) \chi_{0u}(0,0)} \right)^2 \times \left( \frac{[\vec{k} \cdot (\vec{k} + \vec{q})]^2}{k^2(\vec{k} + \vec{q})^2} \right). \quad (4.16)$$

All the  $q$  dependence occurs explicitly in the final term in large parentheses, whose expansion to second order in  $q$  is  $1 - (\vec{q} \times \vec{k}/k^2)^2$ . Thus (4.16) contributes only to  $Z_t$  as expected, and involves only the quantities which led to (4.6) and (4.7) [(4.16 with the final term in large parentheses expanded is the same as (4.1) and (4.2) substituted into (3.53), except for the dimensionless notation used in the latter case]. Thus (4.6) and (4.7) are exact results.

The fact that such a large fraction of the total contribution to  $Z$  comes from this universal region at small  $k$  gives us confidence in approximations such as that of this paper or that of RG, where the fluctuation process that contributes to this region is treated correctly. Other approximations to the gradient coefficient, which either ignore this process or fail to treat it carefully, must be regarded with suspicion.

We conclude this section by mentioning that the width of the peak at small  $k$  is of the order  $\omega_p/v_F$  or  $s/\sqrt{3}$  in units of  $x = k/2k_F$ . Integrating, we find

$$Z \sim \int_0^{s/\sqrt{3}} Z(0) dx = \left( \frac{4\sqrt{3}}{s} \right) \left( \frac{s}{\sqrt{3}} \right) = 4.$$

This estimate gives the correct density dependence for  $Z$  (which according to our calculations is roughly constant), although it over estimates the magnitude by a factor of 3 or 4, principally because the true value of  $Z(x)$  falls off sharply with increasing  $x$ , rather than remaining constant up to a cutoff.

## V. APPLICATION TO MODEL METALLIC SURFACES

We have previously<sup>1,2</sup> discussed the wave-vector decomposition of the exchange-correlation energy of a metallic surface. Using the same notation (except that in the present work we use  $k$  where  $K$  was used before) we define this wave-vector decomposition  $\gamma(k)$  such that the exchange-correlation energy per unit area is given by Eq. (2.12). Here we will generally express  $\gamma$  as a function of the dimensionless variable  $x_B = k/2k_{FB}$ , where  $k_{FB}$  is the bulk Fermi wave vector deep in the metal. We define  $\delta\gamma$  by the relation  $\gamma \equiv \gamma_L + \delta\gamma$ , where  $\gamma_L$  is the local-density approximation to  $\gamma$ .

For large  $k$  we showed that  $\gamma - \gamma_L$  or  $\delta\gamma \rightarrow 0$ , while for small  $k$  we derived the exact form

$$\gamma(\vec{k}) = \frac{\hbar_{\text{FB}}}{4\pi} (\omega_s - \frac{1}{2}\omega_p) \left( \frac{4}{\pi} (k_x^2 + k_y^2)^{1/2} \right), \quad (5.1)$$

where  $k_x$  and  $k_y$  are the components of  $\vec{k}$  parallel to the surface. Upon averaging over the direction of  $\vec{k}$ , (5.1) becomes just Eq. (2.13). We also showed that  $\gamma_L \propto k^2$  at small  $k$ , so that the form (2.13) is contained in  $\delta\gamma$ , with  $\gamma_L$  becoming negligible. In dimensionless units of wave vector, and cgs units (erg/cm<sup>2</sup>) for  $\gamma$ , we find that (2.13) becomes

$$\delta\gamma(x_B) = (3.27 \times 10^5 / \gamma_s^{7/2}) x_B, \quad (5.2)$$

where  $r_s$  corresponds to a point deep in the bulk. The wave-vector decomposition of the gradient coefficient provides another expression ( $\delta_{\text{gr}}\gamma$ ) which can be compared with (5.2) at small  $x_B$ , and with our interpolation scheme at intermediate  $x_B$ .

When averaged over the direction of  $\vec{k}$ , Eq. (2.14) gives

$$\delta_{\text{gr}}\gamma = \frac{4\pi k^2 (2k_{\text{FB}})}{(2\pi)^3 A} \int d^3r B_k^{\text{xc}}(n(\vec{r})) [\vec{\nabla}n(\vec{r})]^2, \quad (5.3)$$

where

$$B_k^{\text{xc}}(n(\vec{r})) = \frac{1}{3} \text{tr} \vec{B}_k^{\text{xc}}(n(\vec{r})) \quad (5.4)$$

and where  $A$  is the area of the surface. We will evaluate (5.3) for model surfaces whose density  $n(\vec{r})$  varies only in one direction (call it the  $z$  direction). Then we have

$$\delta_{\text{gr}}\gamma = \frac{k^2 (2k_{\text{FB}})}{2\pi^2} \int_{-\infty}^{\infty} dz B_k^{\text{xc}}(n(z)) \left( \frac{\partial n}{\partial z} \right)^2. \quad (5.5)$$

Now introduce dimensionless variables  $\bar{z} = k_{\text{FB}} z$  and  $\bar{k}_F = k_F / k_{\text{FB}} = [n(z)/n(\infty)]^{1/3}$  where  $k_F$  is the local Fermi wave vector (a function of  $z$ ) and  $k_{\text{FB}}$  is the bulk Fermi wave vector  $k_{\text{FB}} = k_F|_{z=\infty}$ . We let  $x = k/2k_F$  and  $x_B = k/2k_{\text{FB}}$ . The decomposition  $\delta_{\text{gr}}\gamma$  then becomes a function of  $x_B$  such that the total gradient contribution to the surface energy is  $\int_0^\infty dx_B \delta_{\text{gr}}\gamma(x_B)$ . We let the parameter  $r_s$  refer to the bulk particle spacing parameter  $(4\pi a_0^3 \gamma_s^3 / 3)^{-1} = n(\infty) = k_{\text{FB}}^3 / 3\pi^2$ . Then according to (3.47)–(3.51), Eq. (5.5) becomes

$$\delta_{\text{gr}}\gamma(x_B) = (2.46 \times 10^3 / \gamma_s^3) I(x_B), \quad (5.6)$$

where

$$I(x_B) = \int_{-\infty}^{\infty} d\bar{z} Z(x) \left( \frac{d\bar{k}_F}{d\bar{z}} \right)^2 \left( \frac{1}{\bar{k}_F} \right)^5. \quad (5.7)$$

Note that  $Z(x)$  is implicitly a function of the local density and hence of  $\bar{z}$ . It also depends on  $\bar{z}$  through its explicit  $x$  dependence:  $x = x_B / \bar{k}_F$  and  $\bar{k}_F = \bar{k}_F(\bar{z})$ . Upon change of integration variables, (5.7) becomes

$$I(x_B) = \int_0^{\bar{k}_F^{\text{max}}} \frac{d\bar{k}_F}{\bar{k}_F} Z\left(\frac{x_B}{\bar{k}_F}\right) P(\bar{k}_F), \quad (5.8)$$

where

$$P(\bar{k}_F) = 9 \sum_i \left| \frac{d\bar{k}_F(\bar{z})}{d\bar{z}} \right|_{\bar{z}=\bar{z}_i}, \quad (5.9)$$

where  $\bar{z}_i$  are all the  $\bar{z}$  values where the function  $\bar{k}_F(\bar{z})$  is equal to the given value  $\bar{k}_F$ . For a typical surface profile, there is generally only one  $\bar{z}_i$  unless a  $\bar{k}_F$  is sufficiently close to unity to be within range of Friedel oscillations;  $\bar{k}_F^{\text{max}}$  is the maximum local Fermi wave vector (in our dimensionless units) and is normally slightly greater than unity.

We expect (5.7) to have a large peak at  $x_B \rightarrow 0$ . This can be inferred analytically. Consider the  $x_B = 0$  limit of (5.7). This involves  $Z(0)$ , which according to (4.6) and (4.7) is given by

$$Z(0) = (4\sqrt{3} / s_B) \bar{k}_F^{1/2}, \quad (5.10)$$

where  $s_B$  is the bulk value of the screening parameter. Therefore

$$I(0) = \left( \int_0^{\bar{k}_F^{\text{max}}} \frac{d\bar{k}_F}{\bar{k}_F^{1/2}} P(\bar{k}_F) \right) \frac{4\sqrt{3}}{s_B}. \quad (5.11)$$

Equation (5.11) is an exact result which holds for any density profile varying in one direction only. To see what it means, consider

$$\int_0^\infty I(x_B) dx_B = \int_0^{\bar{k}_F^{\text{max}}} d\bar{k}_F \left( \int_0^\infty dx Z(x) \right) P(\bar{k}_F). \quad (5.12)$$

We know from our previous calculations that  $\int_0^\infty dx Z(x)$  does not vary very much with density and for estimates can be approximated by its high density limit of  $\sim 1.2$ . We are left with two integrals (5.11) and (5.12) whose integrands differ only by a factor of  $\bar{k}_F^{1/2}$ . Remembering that  $\bar{k}_F \propto n^{1/3}$ , we have  $\bar{k}_F^{1/2} \sim n^{1/6}$  whose density variation is hardly worth considering, and we set  $\bar{k}_F^{1/2} \cong 1$  which is obviously a slight overestimate. We therefore have

$$\frac{\delta_{\text{gr}}\gamma(0)}{\int_0^\infty dx_B \delta_{\text{gr}}\gamma(x_B)} = \frac{I(0)}{\int_0^\infty I(x_B) dx_B} \approx \frac{4\sqrt{3}}{1.2 s_B} \approx \frac{15}{r_s^{1/2}}. \quad (5.13)$$

Thus the gradient approximation wave-vector decomposition  $\delta_{\text{gr}}\gamma(x_B)$  has a value at small  $x_B$  which is many times larger than the integrated value. In other words, one might say that to zeroth approximation the wave-vector decomposition of the gradient approximation consists of a sharp peak at zero wave vector, whose width is  $r_s^{1/2}/15$  (in units of  $2k_{\text{FB}}$ ). This conclusion holds for all reasonable density profiles, although the peak width should be slightly profile dependent. These results

should be contrasted with the exact decomposition for a surface (2.13) which vanishes linearly at small wave vector.

To make more quantitative statements the integral in (5.8) must be evaluated. For a first trial we chose a Fermi function density profile

$$n(\bar{z}) = n(\infty)(1 + e^{-\Theta \bar{z}})^{-1}, \quad (5.14)$$

where  $\Theta$  is a dimensionless parameter. This profile has nothing to recommend it except simplicity: It leads to

$$P(\bar{k}_F) = 3\Theta \bar{k}_F (1 - \bar{k}_F^3), \quad (5.15)$$

which allows the integral (5.8) to be done easily, even with the distributional singularities in  $Z$ , which now occur at  $\bar{k}_F = x_B$ . The results are shown in Fig. 7. Note first the large peak at  $x_B = k/2k_{FB} \approx 0$ . Clearly the overwhelming majority of the contribution comes from this peak, as expected from our approximate analysis. Note also that our expectation concerning the effective "weakness" of the apparently extremely singular structure at  $k = 2k_F$  ( $x = 1$ ) is also fulfilled: The only remnant of this structure is a simple discontinuity of very small magnitude. Furthermore, it is clear that the contribution is small everywhere, except for small  $k$ , as we assumed earlier in our interpolation scheme.

The curve shown is for  $\Theta = 1$ , which corresponds to a slower density variation than that in a typical metal. For comparison we show the exact small- $k$  asymptote.<sup>1,2</sup> As the wave vector is decreased, it is clear that the correct wave-vector decomposition must bend downward and join this asymptote; instead the gradient approximation crosses it, curves further upward, finally reaching the large constant  $\delta_{gr}\gamma(0)$  calculated earlier [Eqs. (5.6) and (5.11)]. The contribution of the cross-hatched region in Fig. 7 is undoubtedly spurious. Of course the exact boundaries of the spurious region cannot be obtained by this simple analysis. Nevertheless,

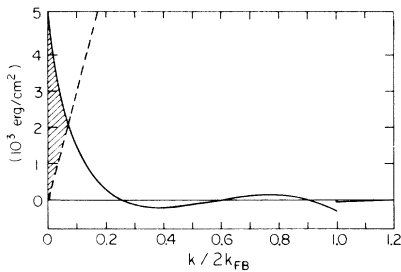


FIG. 7. Wave-vector decomposition of the gradient component of the surface energy  $\delta_{gr}\gamma$  for the "Fermi-function" density profile. The bulk density corresponds to  $r_s = 2.07$ . The broken line is the exact asymptote.

such a large fraction of the total contribution comes from the cross-hatched region, even for a very slowly varying density, that it is difficult indeed to give any credence to the validity of the gradient approximation for surfaces, or other systems whose densities vary at comparable rates.

The parameter  $\Theta$  in (5.14) is proportional to a typical density gradient. For this simple model profile, the results of using other values (and hence other typical density gradients) can be gleaned without further calculation. This is because the only  $\Theta$  dependence in the calculation occurs in (5.15) as a factor which multiplies the final result. Thus the wave vector decomposition for an arbitrary  $\Theta$  is just  $\Theta$  times that shown.

This gives us a clear indication of how the gradient approximation becomes exact in the slowly varying limit. It is clear from examination of the figure, however, that the density gradient must be very small indeed before the contribution from the cross-hatched region becomes negligible.

Two points are in order. First, the failure of the gradient decomposition to vanish as  $k \rightarrow 0$  might be restated as the failure of an electron plus its "exchange-correlation hole" to attain electrical neutrality within a finite radius. This in itself, however, is *not* an indictment of the gradient expansion, because the numerical importance of this failure becomes, as we have seen, less and less important as the gradient in density becomes smaller. The gradient expansion is a rigorous one, which must become valid if the density variation is sufficiently slow. What seems to doom the approximation to failure in practice is that such an unexpectedly large fraction of the total contribution comes from the small- $k$  region, so that the density gradient must be very small indeed for the approximation to be valid. The second point is that for a surface, the exact small- $k$  form (2.13) is *larger* than it would be for other systems where the density gradients are localized. The nonanalytic term  $(k_x^2 + k_y^2)^{1/2}$  in (5.1) arises from the infiniteness of a planar surface plus the long range of the Coulomb interaction. For a localized density gradient, the exact small- $k$  form must vanish as an analytic function of the components of  $\bar{k}$ , and hence at least quadratically. For such a system then the exact small- $k$  form is even *smaller* than for a surface. Nevertheless the gradient coefficient still has a peak at small  $k$  which presumably still translates into a peak at small  $k$  in  $\delta_{gr}\gamma$ . The above suggests that the surface case is actually a (relatively) favorable one for the gradient approximation and that for systems with localized density gradients it is even worse. We note that the result (5.13) is easily generalized to an arbitrary density distribution and may be used to derive a criterion

for the validity of the gradient approximation. This is shown in Appendix C.

Return now to the surface case. So far our conclusions are based on a "Fermi-function" density profile, which is very unphysical. For example, the profile is symmetric about its midpoint, it has no Friedel oscillations, and the  $P(\bar{k}_F)$  function associated with it scales with  $\Theta$  (a property which one would expect only in the slowly varying limit). In short, since the model profile cannot be reasonably fitted to a physical profile, one could never be sure what value of  $\Theta$  corresponded to a real system. We also had the nagging fear that the oscillations about the bulk density in real materials would beat against the distributional singularities near  $2k_F$  so as to produce a substantial contribution in the intermediate- $k$  range.

Therefore we have evaluated (5.8) for a model which has previously been found to give good fits to realistic profiles. This is the linear potential model, whose profile has been evaluated by Sahni *et al.*<sup>21</sup> Its wave functions are the eigenfunctions of  $-\nabla^2 + u(z)$  where  $u(z) = -k_{FB}^2 z / y_F$  for  $z < 0$  and zero otherwise, where  $y_F$  is a dimensionless parameter which determines how fast the density varies. We found previously that  $y_F \sim 3.5$  corresponds roughly to the correct density variation for high density metals ( $r_s \sim 2$ ). Large  $y_F$  implies a slow density variation while small  $y_F$  a fast variation;  $y_F = 0$  is the infinite barrier model, whose exact RPA solution is known.<sup>2,12</sup>

Therefore  $\delta_{gr}\gamma(x_B)$  was calculated for this model from (5.6), (5.8), and (5.9). As before the function  $P(\bar{k}_F)$  [Eq. (5.9)] was a smooth uninteresting function, except that now it has a sharp (but weak) peak near  $\bar{k}_F = 1$  due to the Friedel oscillations. When  $x_B \sim 1$ , the highly singular structure of  $Z$  coincides with this in the integral (5.8). This meant that considerable care had to be taken in performing the integral (5.8).

The term which caused the wildest variations was the  $\delta'$  function term in (3.54a):

$$[3(1 + s^2/2)]^{-1} \delta'(x - 1). \quad (5.16)$$

Since this term integrates to zero when the integral over  $x_B$  is done (that is, when the total gradient contribution rather than the wave-vector decomposition is to be calculated), we omitted it in the Fig. 4 shown in our previous Letter.<sup>10</sup> It is shown in more detail in Fig. 8 here (the broken line). The very sharp, but also weak peak near  $k \sim 2k_{FB}$  is a reflection of the corresponding peak in  $P(\bar{k}_F)$  due to the Friedel oscillations. There is, as in the Fermi-function case, a small simple discontinuity which occurs at a  $k$  corresponding to the largest local  $\bar{k}_F$  value (slightly greater than  $k_{FB}$ ). The solid curve shows what happens when the  $\delta'$

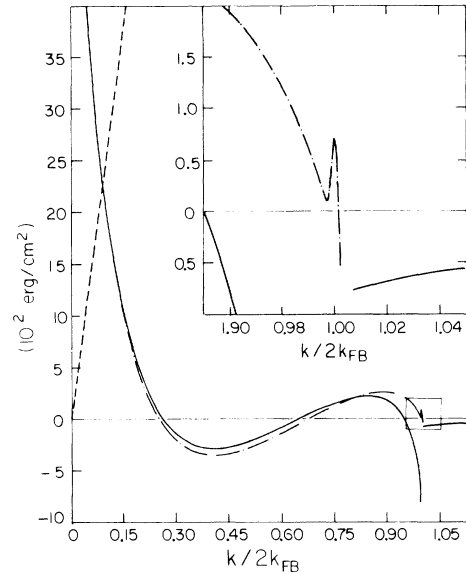


FIG. 8. Wave-vector decomposition  $\delta_{gr}\gamma$  for the linear potential model, with  $r_s = 2.07$  (bulk density parameter) and  $y_F = 3.5$ . The solid curve is the full decomposition (with the rapidly varying piece near  $k = 2k_{FB}$  omitted). The broken curve shows the same (even in the vicinity of  $k = 2k_{FB}$ ), but with the  $\delta'$  function everywhere subtracted out of  $Z$ . The inset shows the detail near  $k = 2k_{FB}$ . The straight dashed curve is as before the exact asymptote.

term (5.16) is included. Near  $\bar{k}_F = 1$  this term is roughly shaped like the convolution of a  $\delta'$  function and the small narrow peak in the broken curve. It is truly too rapidly varying to plot on a graph of reasonable scale, although the negative drop of the solid curve near  $2k_{FB}$  is its precursor. There is thus a rapid variation in the gap of the solid curve. The magnitude of the area under it must be equal to the difference between the areas under the part of the solid curve shown and the broken curve; this is small by inspection. Therefore the contribution of the unplotable section of the curve is small. This conclusion was also verified by direct integration of the unplotable section of the curve. Therefore after much agony we are able firmly to conclude that the anomalies at  $2k_F$  do not contribute any structure of numerical significance. The remaining curves in this paper are shown with the  $\delta'$  term included, and with a slight gap around  $k = 2k_{FB}$ ; it should be understood that this gap contains the weak but rapidly varying structure mentioned above.

We have evaluated the wave-vector decomposition  $\delta\gamma$  in the gradient approximation in the linear potential model for  $y_F = 0.5, 3.5,$  and  $8$  for  $r_s = 2.07$  and  $4$ . The results are shown in the lower portions of Figs. 9 and 10 (a portion of the  $r_s$

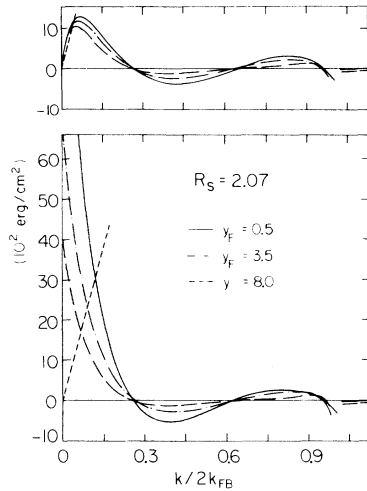


FIG. 9. Lower section:  $\delta\gamma$  in the gradient approximation for the linear potential model for  $r_s = 2.07$ ; solid curve— $y_F = 0.5$ , dot-dash curve— $y_F = 3.5$ , long dashed curve— $y_F = 8$ , short dashed line—exact asymptote. Upper section:  $\delta\gamma$  in the average slope approximation with  $\rho = 1.2$  and Gaussian averaging for the linear potential model  $r_s = 2.07$ . Key to curves as above.

$= 2.07$  curves were shown in our earlier Letter<sup>10</sup>). There seem to be no vast differences between these results and those for the Fermi-function profile. Although we no longer have the scaling property of the latter profile, the curves clearly increase in magnitude in rough proportion to some sort of average density gradient. But now we have a clear idea of what each curve means. For example, at  $r_s \sim 2$ ,  $y_F = 3.5$  corresponds to roughly a real metal;  $y_F \approx 0.5$  is a very rapidly varying profile, which almost corresponds to the infinite barrier model;  $y_F = 8$  is a very slowly varying profile, which corresponds to  $|\nabla n|/2k_F n \sim 0.1$  at the jellium edge.

Again we have plotted the exact asymptotic form

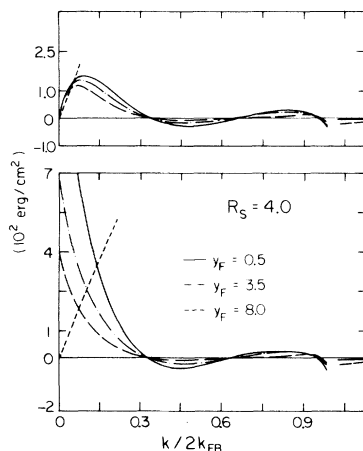


FIG. 10. Same as Fig. 9 but with  $r_s = 4.0$ .

on the same graph. The conclusion is again unmistakable. For the physical case<sup>22</sup>  $y_F = 3.5$  well over half the area is in the “spurious” region. Earlier<sup>8</sup> we made the intuitive remark: “[the value of 0.1 for  $|\nabla n|/2k_F n$  in the  $y_F = 8$  case] is small enough that the accuracy of the gradient correction cannot be doubted.” Clearly we were wrong; the density gradient must be much smaller for the approximation to work. It is thus difficult to imagine a physical situation where the gradient approximation can be accurately applied.

#### VI. GENERALIZATION OF THE GRADIENT APPROXIMATION: A METHOD THAT WORKS

The basic physics behind the gradient approximation is correct. It fails in most practical situations because of the magnitude of the small- $k$  peak. However, the peak itself is also a real physical effect. As we have seen it is produced by long-wavelength excitations (becoming plasmons as  $k \rightarrow 0$ ) which travel parallel to the surface (or more generally, perpendicular to the density gradient) and repeatedly scatter off of it; the long range of the Coulomb interaction causes this process to make an unusually large relative contribution, which increases rapidly as the wave vector is reduced.

We can estimate the dependence on slope (density gradient) of the contribution to the energy of the above process as follows: Consider a surface whose density gradient has a mean slope  $S$ , and which has a characteristic width  $d$ . Let there be an excitation of spatial extent  $l$  located somewhere in the region of the surface (see Fig. 11), and assume that  $l < d$ . In the local-density approximation this excitation propagates as in the bulk,

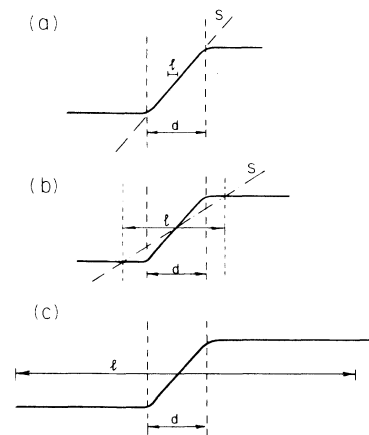


FIG. 11. Schematic illustration of average slope scheme. The quantity  $l$  represents the physical extent of an excitation. (a) Average slope = local slope; (b) Average slope  $\neq$  local slope; gradient approximation fails; (c) Region where exact asymptotic form valid.

going from one density region to another adiabatically. It may scatter in a nonlocal theory and to lowest order in  $S$  (second-order perturbation theory), it makes a contribution  $\sim S^2$  to the exchange-correlation energy. The fraction of the total modes subject to this extra scattering is proportional to the width  $d$  of the surface region, so that the nonlocal part of the surface energy due to excitation of this physical size is  $S^2 d$ . Since  $d \propto 1/S$  for a given bulk density and reasonable surface profile, it follows that this nonlocal surface energy is proportional to  $S$ . This is consistent with Eq. (5.9) which contains one derivative of the density. We shall let such modes within the surface region be called "gradient modes."

Now consider a gradient mode of spatial extent  $l$  a little greater than  $d$ , as pictured in Fig. 11(b). It is unreasonable to suppose that its contribution to the energy is still proportional to the local slope  $S$  at its center, but seems physically reasonable to suppose still that its energy should rather be proportional to some sort of average slope  $\langle S \rangle$  where the average extends over the extent of the excitation. Finally, consider an excitation whose spatial extent is much greater than  $d$ , as pictured in Fig. 11(c). In this limit the excitation becomes an ordinary long-wavelength surface mode, which becomes entirely a surface plasmon at very long wavelength. In this region the nonlocal component of the surface exchange-correlation energy is not related in any simple way to a local slope or average slope. This is the region where the exact small- $k$  form is applicable ( $l \sim 1/k$ ).

If the profile were infinitely slowly varying, then as  $k$  decreased ( $l$  increased) we would remain in the region of Fig. 11(a) essentially forever; the nonlocal component of the wave-vector decomposition of the surface exchange-correlation energy [call it  $\delta_{nt} E_{xc}(\vec{k})$ ] would remain dominated by the gradient mode, and would continue to rapidly increase as  $k$  was lowered. However, for a typical surface profile of a real material, one reaches the crossover between the regions at a finite  $k$ . In the long-wavelength region [Fig. 11(c)]  $\delta_{nt} E_{xc}(k)$  still rises but only as  $|k|^{-1}$ , and thus less rapidly than in the region of Fig. 11(a). (Since the number of modes per unit  $k$  drops as  $k^2$ , this gives a drop in  $\delta\gamma$ , which is proportional to  $k^2 |k|^{-1} = |k|$  in this region [see Eq. (2.13)].)

To improve the gradient approximation we are again faced with an interpolation as in Refs. 1 and 2. There we had little more to guide us than an educated eyeball and a knowledge of the Fermi-Thomas length. Now we know the deviation from the local approximation both above and below the region of interpolation [the region of Fig. 11(b)]. In addition the average slope  $\langle S \rangle$  concept discussed

earlier provides us with a physical (albeit non-rigorous) method for effecting the interpolation.

For simplicity [see Eq. (5.9)] we use the local Fermi level  $\bar{k}_F$  as the fundamental variable instead of density. What we will do is to replace the slope  $d\bar{k}_F/d\bar{z}$  in (5.9) by some sort of average slope where the average extends over the size  $l \sim 1/k$  of the excitation. We define an average derivative:

$$\left\langle \frac{d\bar{k}_F}{d\bar{z}} \right\rangle \equiv \int_0^\infty F(h) \frac{\bar{k}_F(\bar{z} + h/2) - \bar{k}_F(\bar{z} - h/2)}{h} dh, \quad (6.1)$$

where  $F(h)$  is a weighting function which satisfies

$$\int_0^\infty F(h) dh = 1, \quad \int_0^\infty h F(h) dh = \bar{l} \equiv 2k_{FB}^{-1} l. \quad (6.2)$$

We have tried two completely different forms for  $F$  which satisfy (6.2) with little difference in results. The forms tried were

$$F(h) = \delta(h - \bar{l}), \quad (6.3a)$$

where  $\delta(h - \bar{l})$  is the Dirac  $\delta$  function, and

$$F(h) = (32/\pi^2 \bar{l}^3) h^2 \exp(-4h^2/\pi \bar{l}^2). \quad (6.3b)$$

One also has the problem of how to relate  $\bar{l}$  to the wave vector  $x_B$  (in reduced units). Since we are dealing with surface plasmons in the small- $k$  limit, we expect that  $\bar{l} \approx 1/x_B$ , because we know that the fields of a surface plasmon fall off as  $e^{-k|z|} = e^{-x_B|z|}$ . We have set  $\bar{l} = p/x_B$  where  $p$  is an adjustable parameter expected to be of order unity. The final value adopted for most of our curves is  $p = 1.2$ , although the results did not seem very sensitive to physically reasonable choices of  $p$ .

One notes that as  $k$  gets large, the generalized derivative becomes automatically the ordinary derivative. Therefore the use of (6.1) in (5.9) becomes exactly the normal gradient expansion at large  $k$ . Hence we do not have to change from one analytic form to another as  $k$  moves from the region of Fig. 11(a) to the region of Fig. 11(b). Before actually carrying out the numerical calculations, we thought it would be necessary to match two different forms in going from the region of Fig. 11(b) to the exact asymptotic region of Fig. 11(c). However, we found after the fact that the average slope concept gave results in the region of Fig. 11(c) that were sufficiently close to the exact asymptote (2.13) that trying to make a better fit was not worth the effort.

No particular attempt was made to get a "best fit" and we are not even sure what criterion should be used for this. The only values of the constant tried were  $p = 1.0, 1.2$ , and  $1.4$  for each of the weighting functions (6.3). The curves for  $p = 1.2$  and the Gaussian weighting function are shown in detail in Figs. 12-14, where we show the  $r_s = 2.07$

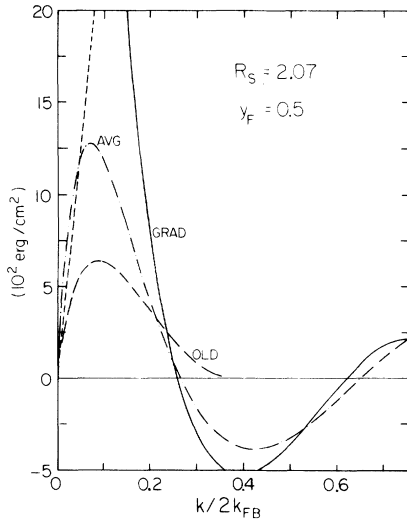


FIG. 12. Wave-vector decomposition  $\delta\gamma$  for the linear potential model with  $r_s = 2.07$  in several approximations. Solid curve—gradient approximation; dot-dash curve—average slope approximation (Gaussian with  $p = 1.2$ ); long-dashed curve—circular interpolation of Refs. 1 and 2; short-dashed line—exact asymptote. Here  $y_F = 0.5$  (a rapidly varying density).

case for  $y_F = 0.5, 3.5,$  and  $8.0$ . Note that at large  $k$  the average slope approximation agrees with the gradient approximation, while at small  $k$  it approaches zero linearly, as the exact form does, but with a different slope. For comparison we also plot the results of our older circular interpolation, which agrees remarkably well except in the rapidly varying  $y_F = 0.5$  case. It is certainly clear in any case that the older interpolation has picked up the major correction to the local approxi-

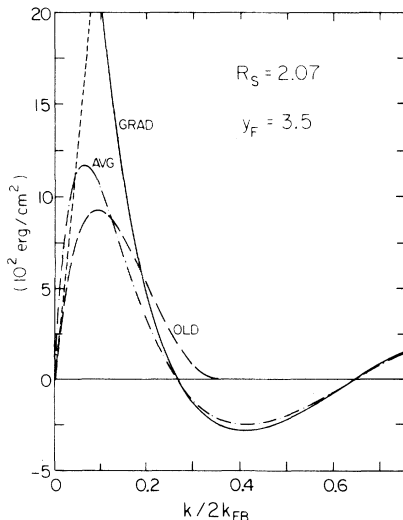


FIG. 13. Same as Fig. 12, except  $y_F = 3.5$  (a density variation typical of real surfaces).

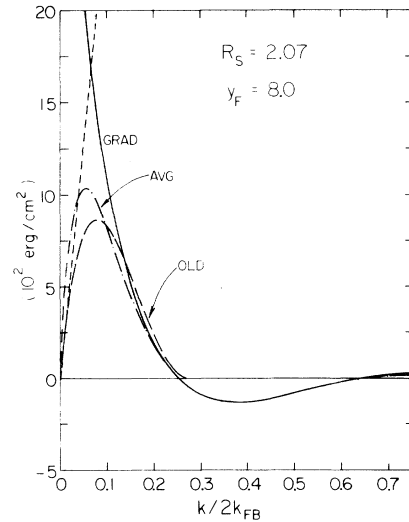


FIG. 14. Same as Fig. 12, except  $y_F = 8.0$  (a slowly varying density).

mation.

In Fig. 15 we illustrate the insensitivity of the results to the exact definition of average slope. We show the results of using both the  $\delta$  function  $F$  [Eq. (6.3a)] and the Gaussian [Eq. (6.3b)] for the various values of  $p$  which we tried. We thought  $p = 1.2$  with Eq. (6.3b) looked best (after looking at computer plots like<sup>23</sup> Figs. 12–14 for all the different possibilities, and checking the integrated area under the  $y_F = 0.5$  cases with the exact in-

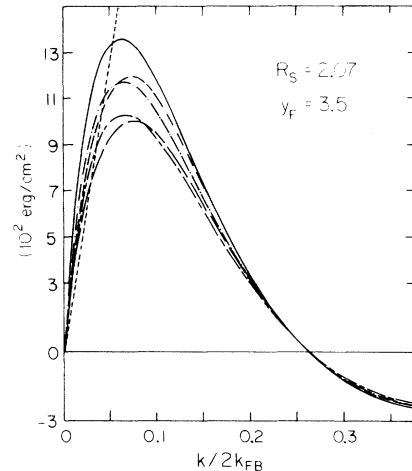


FIG. 15. Comparison of different methods for calculating the average slope. All curves are the linear potential model with  $r_s = 2.07$ ,  $y_F = 3.5$ . Solid curve—Gaussian,  $p = 1.0$ ; medium dashed curve—delta function,  $p = 1.0$ ; dot-dash curve—Gaussian,  $p = 1.2$ ; long-dashed curve—delta function,  $p = 1.2$ ; alternating long and short dashes—Gaussian,  $p = 1.4$ ; short dashed line—exact asymptote.

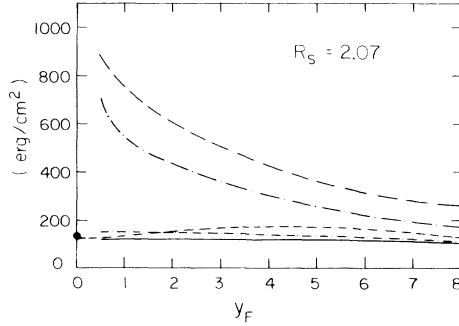


FIG. 16. Nonlocal contribution to the surface exchange correlation energy in various approximations for a linear potential profile with  $r_s = 2.07$  as a function of the slope parameter  $y_F$ . Long dash—gradient approximation of present paper; long dot-dash—gradient approximation of Ref. 6; short-dash—circular interpolation of Refs. 1 and 2; short dot-dash—Gaussian average slope approximation,  $p = 1.0$ ; solid—Gaussian average slope,  $p = 1.2$ . A physical profile corresponds to  $y_F \sim 3.5$ . The solid dot at  $y_F = 0$  is the exact calculation of Ref. 12.

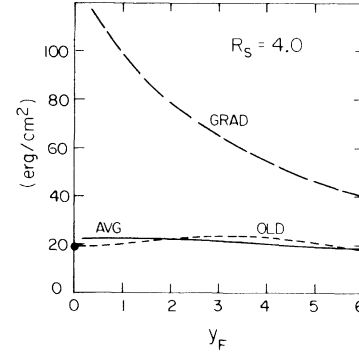


FIG. 17. Nonlocal contribution to the surface exchange correlation energy in various approximations for a linear potential profile with  $r_s = 4.0$  as a function of  $y_F$ . Long dashes—the gradient approximation of the present paper; short dashes—the circular interpolation of Refs. 1 and 2; solid—Gaussian average slope approximation,  $p = 1.2$ . A physical profile corresponds to  $y_F \sim 2$ . The solid dot at  $y_F = 0$  is the exact calculation of Ref. 12.

finite barrier model results,<sup>2,12</sup> but we do not have any strong reason for preferring it to the others.

We also made calculations for  $r_s = 4$ . These are shown only for the Gaussian  $F$  and  $p = 1.2$  in the top half of Fig. 10 for easy comparison with the gradient approximation curves; similar results for  $r_s = 2.07$  are shown in the top part of Fig. 9.

In Fig. 16 (which is a more complete version of the inset in Fig. 4 of Ref. 10) and in Fig. 17 we show the integrated area under the wave-vector decomposition  $\delta\gamma(x_B)$  in the average slope scheme, that is, the total nonlocal contribution to the surface energy in this approximation, and compare it with other approximations. Note that results for different values of  $p$  are in reasonable agreement with each other, and also with the circular interpolation scheme. They also are very consistent with the exact results as  $y_F \rightarrow 0$ . They differ substantially, however, from two versions of the gradient approximation.

The Gaussian average slope scheme we have been discussing is a nonlocal-density functional for the exchange-correlation energy, which could be generalized to arbitrary three-dimensional density variation. The exact form of it is tractable, but probably too complex for widespread practical application.

There is another approach to correcting the local-density approximation which may have promise (at least for systems of nearly uniform density). Note that if we define

$$K_k^{xc}(\vec{r} - \vec{r}') = \int \frac{d^3q}{(2\pi)^3} e^{i\vec{q} \cdot (\vec{r} - \vec{r}')} K_{xc}(\vec{k}, \vec{q}), \quad (6.4)$$

where  $K_{xc}(\vec{k}, \vec{q})$  is given by (2.45), then  $K_k^{xc}(\vec{r} - \vec{r}')$  is the *wave-vector composition* of the  $K^{xc}$  coefficient defined by Kohn and Sham<sup>3</sup> in their Eq. (A22). Numerical evaluation of our expression for  $K_{xc}$  and then finding an analytic approximant to it does not seem out of the question.

## APPENDIX A: ANALYTIC EXPRESSIONS

### 1. Analytic expressions for the $\lambda$ 's

The various quantities  $\lambda$  as defined by (3.17)–(3.19), combined with (3.11)–(3.13), were evaluated by substitution of (3.7)–(3.10). One finds

$$\lambda_0 = -(1/x) \ln(a/b), \quad (A1)$$

where  $a = y^2 + (1-x)^2 x^2$  and  $b = y^2 + (1+x)^2 x^2$ . Similarly

$$\lambda_1 = \frac{1}{2} x^{-2} \ln(a/b) - (1-2x)(1-x)/a + (1+2x)(1+x)/b, \quad (A2)$$

$$\lambda_2^t = (2x/3)[(1-x)/a - (1+x)/b], \quad (A3)$$

and

$$\lambda_2^t = -(3x)^{-1} \left\{ [(1-x)^2(2x-3) - x(1-x)]/a + [(1+x)^2(2x+3) - x(1+x)]/b \right. \\ \left. - (1-2x)^2(a-2y^2)/a^2 + (1+2x)^2(b-2y^2)/b^2 + (3/2x^2) \ln(a/b) \right\}. \quad (\text{A4})$$

## 2. Analytic expressions for the $w$ 's

The quantities  $w$  are defined by (3.14)–(3.16) in conjunction with (3.5) in terms of  $\mathcal{U}$  and  $D$ .  $\mathcal{U}$  is given by (2.46) and (2.38), where again  $\chi_{0w}$  of (2.38) is given by (3.7)–(3.9). (Note that  $P \equiv \chi_{0w}$ .) Similarly  $D$  is given in terms of the same quantities by (2.47). Expanding all quantities to second order in  $q$  yields expressions for  $w$  in terms of the quantities defined below. First let  $\mathcal{P} \equiv VP \equiv V\chi_{0w}$ , so that  $\epsilon = 1 - \mathcal{P}$ . Carrying out the integrals in (3.7) gives

$$\mathcal{P} = -(s^2/x^2) \left( \frac{1}{2} + x^2 \mathcal{F} \right), \quad (\text{A5})$$

where

$$x^2 \mathcal{F} = \left\{ -[y^2 + x^2(1-x^2)]/(8x^3) \ln(a/b) - (y/2x) \mathcal{F}_2 \right\}, \quad (\text{A6})$$

and where

$$\mathcal{F}_2 = \tan^{-1}[x(1-x)/y] + \tan^{-1}[x(1+x)/y]. \quad (\text{A7})$$

Defining  $\mathcal{P}_x, \mathcal{F}_x, \mathcal{P}_{xx}, \mathcal{F}_{xx}$  to be the respective first and second derivatives (with respect to  $x$ ) of the indicated-quantities we obtain

## 3. Expression for the $b$ 's (and $\tilde{h}$ )

The quantities  $b_2^t$  and  $b_2^t$  as defined by (3.24), (3.25), and (3.29) were evaluated by substitution of (3.7)–(3.10) into (3.27). One obtains

$$b_2^t = \frac{16}{3} \left\{ (1-2x)^2 x(1-x)(a-4y^2)/(2a^3) - (1+2x)^2 x(1+x)(b-4y^2)/(2b^3) + (1+4x^2)(a-2y^2)/(4xa^2) \right. \\ \left. - (1+4x^2)(b-2y^2)/(4xb^2) + x(1-x)/a - x(1+x)/b \right\} \quad (\text{A12a})$$

and

$$\delta_2^t = \frac{16}{3} \left[ x(a-2y^2)/a^2 - x(b-2y^2)/b^2 \right. \\ \left. + x(1-x)/a - x(1+x)/b \right]. \quad (\text{A12b})$$

Because of the change in contours between (3.30) and (3.25), the quantity  $\tilde{h}_2$  is not simply a rescaled version of  $\tilde{H}^{(2)}$ , but is nevertheless easily evaluated and we find

$$\tilde{h}_2 = 16\pi/3x^2. \quad (\text{A13})$$

## 4. Chemical potential shift term

Here we list  $\bar{b}_2$  and  $\bar{c}_2$  as defined by (3.35)–(3.37), which are easily worked out by expanding  $J_q^+$  of Eq. (3.32) in powers of  $q$ , performing the  $\mu$  deriva-

$$\mathcal{P}_x = -s^2(-x^{-3} + \mathcal{F}_x), \quad (\text{A8a})$$

$$\mathcal{P}_{xx} = -s^2(3/x^4 + \mathcal{F}_{xx}), \quad (\text{A8b})$$

$$\mathcal{F}_x = -5\mathcal{F}/x + \mathcal{G}, \quad (\text{A8c})$$

$$\mathcal{F}_{xx} = 5\mathcal{F}/x^2 - 5\mathcal{F}_x/x - 5\mathcal{G}/x + \mathcal{K}, \quad (\text{A8d})$$

where

$$\mathcal{G} = -\frac{1}{4} x^{-4} [4y\mathcal{F}_2 + (1-2x^2) \ln(a/b) - 2x] \quad (\text{A9})$$

and

$$\mathcal{K} = -\frac{1}{4} x^{-5} [4y\mathcal{F}_2 + (1-6x^2) \ln(a/b) + 4x \\ + 2x^2(1-x)(1-2x)^2/a \\ - 2x^2(1+x)(1+2x)^2/b]. \quad (\text{A10})$$

One then obtains

$$w_0 = (x^2\epsilon)^{-1}, \quad (\text{A11a})$$

$$w_1 = (-2/x^3 + 2\mathcal{P}_x/3\epsilon x^2)/\epsilon, \quad (\text{A11b})$$

$$w_2^t = [3/x^4 - (4/3\epsilon x^3)\mathcal{P}_x + (1/3\epsilon x^2)\mathcal{P}_{xx} \\ + (1/2\epsilon^2 x^2)\mathcal{P}_x^2]/\epsilon, \quad (\text{A11c})$$

$$w_2^t = [-x^{-4} + (3\epsilon x^3)^{-1}\mathcal{P}_x]/\epsilon. \quad (\text{A11d})$$

tives indicated, and comparing with (3.35). We find

$$\bar{b}_2 = -\frac{16}{3} [(1-\epsilon)/2x] \ln(a/b) \quad (\text{A14})$$

and

$$\bar{c}_2 = -\frac{16}{3} \pi [(1-x)/x^2] \Theta(1-x), \quad (\text{A15})$$

where  $\Theta(\xi)$  is the unit step function.

## APPENDIX B: POLYNOMIAL FIT TO GRADIENT COEFFICIENT

Here we give an analytic polynomial fit to our expression for the gradient coefficient  $B_{xc}$  which was plotted in Ref. 10. Let  $y = (n^{4/3}/e^2)B_{xc}(10^3)$  and

$x$  be the local value of  $r_s$ . For  $x=0$  our results agree exactly with the exact high-density results.<sup>5</sup> ( $y=2.568$ .) The analytic expression below fits our calculation for  $1 < x < 12$ . We find

$$y = y_1 \left(1 - \frac{x}{x_1}\right) \left(1 - \frac{x}{x_2}\right) \left(1 - \frac{x}{x_3}\right) + y_2, \quad (\text{B1})$$

where  $y_1=0.155$ ,  $y_2=2.50$ ,  $x_1=-4.4$ ,  $x_2=8.2$ , and  $x_3=21.5$ .

#### APPENDIX C: AN ESTIMATE OF THE VALIDITY OF THE GRADIENT APPROXIMATION IN THE GENERAL CASE

In Sec. V we gave an argument based on an exact limit that the contributions to the gradient approximation for the energy all arise from a small-wave-vector region about the origin. Here we make this argument general for any type of density variation.

According to (2.14) the gradient contribution to the exchange-correlation energy for an arbitrary density variation is

$$\delta_{\text{gr}} E_{\text{xc}} = \int \frac{d^3 k}{(2\pi)^3} \int d^3 r \langle B_k^{\text{xc}}(n(\vec{r})) \rangle [\vec{\nabla} n(\vec{r})]^2. \quad (\text{C1})$$

We wish to normalize its wave-vector decomposition  $\delta_{\text{gr}} E_{\text{xc}}(k)$  so that  $\int_0^\infty dk \delta_{\text{gr}} E_{\text{xc}}(k) = \delta_{\text{gr}} E_{\text{xc}}$ . Then according to (3.47) and (3.51)

$$\delta_{\text{gr}} E_{\text{xc}}(k) = \int d^3 r \frac{(\nabla n)^2}{n^{4/3}} \frac{\bar{\alpha} Z(k/2k_F)}{2k_F}, \quad (\text{C2})$$

where  $\bar{\alpha} = \pi e^2 / 16(3\pi^2)^{4/3}$ . For  $k=0$ , (4.6) and (4.7) imply that

$$Z(0) = (4\sqrt{3}/k_{\text{FT}}) 2k_F, \quad (\text{C3})$$

where  $k_{\text{FT}}$  is the local Fermi-Thomas wave vector. Therefore

$$\begin{aligned} \delta_{\text{gr}} E_{\text{xc}}(0) &= \int d^3 r \frac{(\nabla n)^2}{n^{4/3}} \frac{\bar{\alpha} 4\sqrt{3}}{k_{\text{FT}}(\vec{r})} \\ &\approx \frac{4\sqrt{3}}{k_{\text{FT}}} \left( \bar{\alpha} \int d^3 r \frac{(\nabla n)^2}{n^{4/3}} \right), \end{aligned} \quad (\text{C4})$$

where, since  $k_{\text{FT}}(\vec{r})$  varies only as the sixth root of  $n$ , we have pulled it out of the integral and replaced it by a "typical" value  $k_{\text{FT}}$ . We may also estimate the integral over wave vector of (C2)

$$\delta_{\text{gr}} E_{\text{xc}} = \bar{\alpha} \int d^3 r \frac{(\nabla n)^2}{n^{4/3}} \left[ \int_0^\infty d\left(\frac{k}{2k_F}\right) Z\left(\frac{k}{2k_F}\right) \right]. \quad (\text{C5})$$

Now, we have found (see previous Appendix of Ref. 10) that the quantity in square brackets is only weakly dependent on density and may be approximately replaced by its high-density limit of  $\sim 1.2$ . Therefore we have

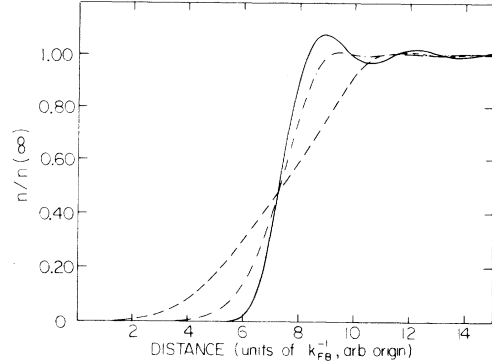


FIG. 18. Density profiles of linear-potential model. Solid curve,  $y_F=0.5$ ; dot-dashed curve,  $y_F=3.5$ ; dashed curve,  $y_F=8.0$ .

$$\frac{\delta_{\text{gr}} E_{\text{xc}}(0)}{\delta_{\text{gr}} E_{\text{xc}}} \approx \frac{4\sqrt{3}}{(1.2)k_{\text{FT}}} \approx \frac{6}{k_{\text{FT}}}. \quad (\text{C6})$$

For a typical material this is numerically equal to 10 or so, and it suggests, independently of the density variation, that roughly the totality of the gradient contribution comes from a narrow region  $k \leq k_{\text{FT}}/6$ .

Since we know that rigorously  $\delta E_{\text{xc}}(k)$  goes to zero either linearly or quadratically with  $k$ , the criterion for the gradient approximation's validity is that the cross over between the latter exact behavior and the behavior predicted by the gradient approximation occur at a wave vector  $k_c$  such that  $k_c \ll k_{\text{FT}}/6$ . Examination of (4.11) suggests that the crossover occurs at  $k_c = q$  where  $q$  is identifiable with  $\nabla n/n$ . Therefore our criterion for the validity of the gradient approximation is that

$$\nabla n/n \ll k_{\text{FT}}/6. \quad (\text{C7})$$

It is the fact that  $k_{\text{FT}}$  is the relevant wave vector rather than  $2k_F$ , plus the conspiracy of numerical factors to produce a 6 instead of unity, that cause the above (correct) criterion to be a whole order of magnitude more severe for typical materials than the more naive (but incorrect) criterion

$$\nabla n/n \ll 2k_F. \quad (\text{C8})$$

We note in conclusion that (C7) is also consistent with the detailed calculations for surfaces that we have made in this paper.

#### APPENDIX D: LINEAR POTENTIAL MODEL

The linear potential model is discussed in Refs. 10 and 21. We present here in Fig. 18 the profiles for the actual  $y_F$  values used in this paper.

## ACKNOWLEDGMENTS

We are grateful to V. Sahni for supplying us with a computer program to generate the profiles of the linear-potential model. We also thank P. Jacques and R. Plano for aid in the use of their group's

interactive computer, which made the evaluation of the various highly singular, multiple-dimensional integrals less a burden than it otherwise would have been. This work was supported in part by the National Science Foundation, Grants Nos. DMR-77-08694 and DMR-78-12398.

<sup>1</sup>D. C. Langreth and J. P. Perdew, *Solid State Commun.* **17**, 1425 (1975).

<sup>2</sup>D. C. Langreth and J. P. Perdew, *Phys. Rev. B* **15**, 2884 (1977).

<sup>3</sup>P. Hohenberg and W. Kohn, *Phys. Rev.* **9**, B864 (1964); W. Kohn and L. J. Sham, *Phys. Rev.* **140**, A1133 (1965).

<sup>4</sup>N. D. Lang and L. J. Sham, *Solid State Commun.* **17**, 581 (1975).

<sup>5</sup>S.-K. Ma and K. A. Brueckner, *Phys. Rev.* **165**, 18 (1968). These authors calculated the correlation term alone; the exchange term was calculated by L. J. Sham, in *Computational Methods in Band Structure*, edited by P. M. Marcus, J. F. Janak, and A. R. Williams (Plenum, New York, 1971).

<sup>6</sup>M. Rasolt and D. J. W. Geldart, *Phys. Rev. Lett.* **35**, 1234 (1975); D. J. W. Geldart and M. Rasolt, *Phys. Rev. B* **13**, 1477 (1976). Abbreviated RG in text.

<sup>7</sup>K.-H. Lau and W. Kohn, *J. Phys. Chem. Solids* **37**, 99 (1976); A. K. Gupta and K. S. Singwi, *Phys. Rev. B* **15**, 1801 (1977); M. Rasolt, J. S.-Y. Wang, and L. M. Kahn, *Phys. Rev. B* **15**, 580 (1977).

<sup>8</sup>J. P. Perdew, D. C. Langreth, and V. Sahni, *Phys. Rev. Lett.* **38**, 1030 (1977).

<sup>9</sup>Some of our results were presented earlier, *Bull. Am. Phys. Soc.* **24**, 439 (1979); at the same meeting we learned through private conversation with M. Rasolt that he and D. J. W. Geldart had nearly completed an independent wave-vector analysis of the gradient coefficient.

<sup>10</sup>The present work is a complete account of the Letter version: D. C. Langreth and J. P. Perdew, *Solid State Commun.* **31**, 567 (1979).

<sup>11</sup>Our earlier interpolation work was criticized by M. Rasolt, G. Malmstrom and D. J. W. Geldart, *Bull. Am. Phys. Soc.* **24**, 438 (1979), on the basis of a wave-vector decomposition of the infinite barrier model including exchange, but *no correlation*. We and others have found (see Refs. 1, 2, and 4) that there is so much cancellation between exchange and

correlation contributions, that calculations based on exchange alone cannot be considered reliable.

<sup>12</sup>E. Wikborg and J. E. Inglesfield, *Solid State Commun.* **16**, 335 (1975).

<sup>13</sup>V. Peuckert, *J. Phys. C* **9**, 4173 (1976).

<sup>14</sup>O. Gunnarsson and B. I. Lundqvist, *Phys. Rev. B* **13**, 4274 (1976).

<sup>15</sup>J. E. Inglesfield and I. D. Moore, *Solid State Commun.* **26**, 867 (1978).

<sup>16</sup>See for example, D. Pines and P. Nozières, *The Theory of Quantum Liquids* (Benjamin, New York, 1966); D. Pines, *Elementary Excitations in Solids* (Benjamin, New York, 1964).

<sup>17</sup>L. P. Kadanoff and G. Baym, *Quantum Statistical Mechanics* (Benjamin, New York, 1962).

<sup>18</sup>E.g., see A. A. Abrikosov, L. P. Gorkov, and I. E. Dzyaloshinski, *Methods of Quantum Field Theory in Statistical Physics*, translated by R. A. Silverman (Prentice-Hall, Englewood Cliffs, N.J., 1963), or Ref. 17.

<sup>19</sup>The quantity  $Z$  is defined so that with respect to scale factors our quantity  $\int_0^\infty Z dx$  corresponds to what RG call  $Z$  in the high-density limit. The difference is that we have included the compressibility terms [the second set of parentheses inside the square brackets in each of Eq. (3.53)] in the definition, while they have not.

<sup>20</sup>If we write  $\bar{\Lambda}_{\vec{k},\vec{q}}$  in terms of symmetric variables  $\vec{k}$  and  $\vec{k}'$  where  $\vec{k}' = \vec{k} + \vec{q}$ , then we expand  $\bar{\Lambda}_{\vec{k},\vec{q}} = a_0 + a_{11}k^2 + a_{12}\vec{k} \cdot \vec{k}' + a_{22}k'^2 + \dots$ . Because  $\omega$  is finite,  $\bar{\Lambda}$  must vanish if either  $k$  or  $k'$  vanishes, so that  $a_0 = a_{11} = a_{22} = 0$ .

<sup>21</sup>V. Sahni, J. B. Krieger, and J. Gruenebaum, *Phys. Rev. B* **15**, 1941 (1977); V. Sahni and J. Gruenebaum, *Solid State Commun.* **21**, 463 (1977).

<sup>22</sup>For  $\gamma_s = 4$ , the physical case corresponds to even a smaller  $y_F$ , roughly half way between our  $y_F = 0.5$  and  $y_F = 3.5$  curves.

<sup>23</sup>Except that the circular interpolation curves had not been calculated in this coordinate system at that time.